# Diamagnetism and neutrals depletion in a plasma

Amnon Fruchtman, and Shunjiro Shinohara

Citation: Physics of Plasmas **24**, 103523 (2017);
View online: https://doi.org/10.1063/1.4997250
View Table of Contents: http://aip.scitation.org/toc/php/24/10
Published by the American Institute of Physics

# Diamagnetism and neutrals depletion in a plasma

Amnon Fruchtman[1] and Shunjiro Shinohara[2]
[1]*Department of Physics, Faculty of Sciences, H. I. T.—Holon Institute of Technology, 52 Golomb Street, Holon 58102, Israel*
[2]*Division of Advanced Mechanical Systems Engineering, Institute of Engineering, Tokyo University of Agriculture and Technology, 2-24-16, Naka-cho, Koganei, Tokyo 184-8588, Japan*

(Received 22 July 2017; accepted 28 September 2017; published online 23 October 2017)

Recent experimental and theoretical findings [Shinohara *et al.*, Phys. Plasmas **23**, 122108 (2016)] regarding the pressure balance between a cylindrical plasma, an axial magnetic field, and neutral gas are explored further theoretically. The length of the cylinder is assumed much larger than its radius, so that axial losses are small and cross-field transport is dominant. Conditions for either magnetic pressure or neutral pressure balancing the plasma pressure and an associated coupling parameter, which were identified in the above-mentioned recent study, are examined further. In addition, a second coupling parameter is identified which determines which is larger, the relative change in the magnetic field or the relative change in neutral density. An unexpected nonmonotonic variation of the plasma density with the plasma particle flux is demonstrated. It is shown that for plasma beta close to unity, as plasma generation and plasma particle flux increase, the plasma density surprisingly decreases. This decrease follows a decrease in plasma confinement due to an increased plasma diamagnetism. The effect of the magnetic field on neutral depletion is examined. It is shown that an increase in the magnetic field as the plasma density is kept constant results in a decrease in neutral depletion, while an increase in the magnetic field as the plasma particle flux is kept constant results in constant neutral depletion. *Published by AIP Publishing.* https://doi.org/10.1063/1.4997250

## I. INTRODUCTION

Interesting nonlinear phenomena are observed in plasmas of high beta (the ratio of plasma pressure to magnetic pressure). Examples include mirror and firehose instabilities,[1] modified waves,[2] and Alfven Ion Cyclotron (AIC) instabilities[3] in laboratory plasmas and magnetic holes in solar wind in space plasmas.[4] Diamagnetism is particularly a fundamental characteristic of high beta plasmas. A large diamagnetic current which modifies the magnetic field is expected to arise.

High temperature/energy plasmas in magnetic fusion devices and in certain plasma thrusters are candidates for reaching high beta, such as the spherical tokamak, Field Reversed Configuration, and MagnetoPlasmaDynamic thruster. However, often the magnetic pressure in high temperature plasmas is high, so that the plasma beta turns out not to be high. Low temperature magnetized plasmas in which the magnetic field is low can be of a high beta value, especially in plasma sources such as the helicon where the plasma density is relatively high.[5] Such low temperature plasmas are expected to be diamagnetic.

Diamagnetic currents and the associated magnetic field modification in low temperature plasmas have indeed been measured (see, for example, Refs. 6–13). Roberson *et al.*[10] measured a large modification of the magnetic field in the plasma plume of a high power helicon. Takahashi and his colleagues described in several publications[11–13] measurements of the magnetic field modification in a helicon plasma thruster. From the modified magnetic field, they evaluated the azimuthal diamagnetic current and calculated the thrust delivered by the magnetic pressure.[11] However, a few publications on high beta helicon plasma sources[6–9] reported magnetic reduction that was much smaller than expected by the plasma beta. Scime *et al.* claimed that because their plasma is not in magnetohydrodynamic equilibrium, the magnetic field is only slightly reduced by the high-beta plasma.[6] Stenzel suggested that a radial electric field is excited which suppresses the diamagnetic current.[7] Corr and Boswell identified magnetic field penetration as the source of low diamagnetism.[8] It is important to explore further the causes of the often observed suppressed diamagnetism.

Suppression of diamagnetism in a low-temperature partially ionized plasma was recently investigated experimentally[14] in the Large Helicon Plasma Device[15] and also in the Large Mirror Device.[16] The reduction of the magnetic field was measured as a function of the magnetic field for various argon gas pressures. The measurements were compared with the calculations by the use of a theoretical model. It was demonstrated through the experiment and the theory that the suppression of the diamagnetic field can be caused by neutral pressure. Neutral depletion by the plasma pressure created a gradient of the neutral pressure that partially balanced the gradient of the plasma pressure instead of the gradient of the magnetic field, and therefore, the diamagnetism became weaker. Thus, in the partially ionized plasma, there is a competition between the magnetic pressure and neutral pressure in balancing the plasma pressure. This competition is reflected in the relative dominance of diamagnetism and neutral depletion. The dominance in balancing the plasma pressure is not determined solely by the magnitudes of magnetic pressure and of neutral pressure but rather by the strength of the coupling of the plasma to the magnetic field relative to the strength of its coupling to the neutrals. The stronger the coupling is the larger the gradient is, and accordingly, the larger is the change across the discharge, either of the magnetic pressure or of the

neutral pressure. In Ref. 14, a parameter was identified which determines which coupling is larger, thus leading to the pressure change that is dominant.

Our purpose here is to explore further theoretically the competition between the magnetic pressure and neutral pressure in balancing the plasma pressure. In Sec. II, we present the theoretical model for the plasma, the neutrals, and the magnetic field in a cylindrical configuration. The length of the cylindrical plasma discharge is assumed much larger than its radius, so that axial end losses are assumed to be small. The discharge is described by a one-dimensional (1D) steady-state model, as radial dynamics is assumed to be dominant. Therefore, the model has to be modified in order to describe helicons in which axial dynamics is dominant. In Sec. III, two parameters that characterize the interaction, $C_1$ and $C_2$, are identified. They are called here coupling parameters although they vary radially across the discharge. The first coupling parameter, $C_1$, is reduced to the coupling parameter that was identified in Ref. 14, which determines which pressure change, that of the magnetic field or that of the neutrals, will balance the plasma pressure. The second coupling parameter, $C_2$, determines which is larger, the relative change in the magnetic field or the relative change in the neutral density. Section IV presents an analytic solution of the linearized equations for low plasma density.

In Sec. V, we calculate the plasma steady-state in two cases in which the neutral pressure and the magnetic pressure are the same. However, the neutral (gas) temperature and density are different in the two cases. As a result, the first of the two coupling parameters has a different size in the two cases. The calculation shows that, although the pressures themselves are the same, in one case, diamagnetism is dominant, while in the other case, neutral depletion is dominant.

In Sec. VI, the role of the second coupling parameter is demonstrated. It is shown how the relative changes in the magnetic field and of the neutral density vary even if magnetic pressure and neutral pressure are fixed. For different gases of such identical pressures, this second coupling parameter is different, resulting in different relative changes of the magnetic field and of the neutral density. Also, demonstrated here a somewhat unexpected effect. It is expected that as the rate of plasma generation increases, the plasma density should increase as well. It is shown that in a certain regime, an increase in the rate of generation results in a decrease in the plasma density, so that there is a nonmonotonic dependence of the plasma density on the rate of plasma generation.

In Sec. VII, we examine the effect of the magnetic field on neutral depletion, not necessarily related to diamagnetism. Neutral depletion has been investigated theoretically extensively over the years (see, for example, Refs. 17–24). It has been recently claimed[24] that neutral depletion gets smaller when the magnetic field increases. It is shown in Sec. VII that neutral depletion indeed gets smaller with the magnetic field if the plasma density is kept constant. However, it is also shown that if the plasma radial particle flux is kept constant, then neutral depletion is hardly affected by the variation of the magnetic field. Finally, conclusions are presented in Sec. VIII.

## II. THE MODEL

We assume an azimuthally symmetric partially ionized cylindrical plasma that is immersed in a magnetic field parallel to the axis of symmetry denoted as the $z$ axis, so that $\vec{B} = \hat{e}_z B$. The length of the cylindrical tube is assumed much larger than its radius $a$, so that radial cross-field transport is dominant and axial transport along field lines is negligible. The short circuit effect[23,25] is also assumed to be negligible and the radial transport is ambipolar. As motion along magnetic field lines is neglected, the problem becomes one-dimensional where all variables depend on $r$ only. The plasma and the neutral gas are assumed to be in the steady-state, so that the equations are time-independent.

Both plasma and neutrals are described by fluid equations. The plasma is described first. The momentum equations in the $r$, $\vartheta$ plane exhibit a force balance for the ions and for the electrons. In the radial direction, there is balance between electric force, magnetic force, pressure gradient, and collisions for the electrons

$$-neE - \frac{\partial(nT_e)}{\partial r} - nev_{e\vartheta}B - nm_e\nu_{eN}(v_r - V_r) = 0, \quad (1)$$

and an equivalent force balance for the ions

$$neE - \frac{\partial(nT_i)}{\partial r} + nev_{i\vartheta}B - nm_i\nu_{iN}(v_r - V_r) = 0. \quad (2)$$

In the azimuthal direction, there is a balance between magnetic force and collisions for the electrons

$$nev_rB - nm_e\nu_{ei}(v_{e\vartheta} - v_{i\vartheta}) - nm_e\nu_{eN}(v_{e\vartheta} - V_\vartheta) = 0, \quad (3)$$

and equivalently for the ions

$$-nev_rB - nm_i\nu_{ie}(v_{i\vartheta} - v_{e\vartheta}) - nm_i\nu_{iN}(v_{i\vartheta} - V_\vartheta) = 0. \quad (4)$$

Here, $T_e$ and $T_i$ are the electron and ion temperatures (in energy units), $n$ is the density of the quasi-neutral plasma, $e$, $m_i$, and $m_e$ are the elementary charge and ion and electron masses, $v_{e\vartheta}$ and $v_{i\vartheta}$ are the electron and ion azimuthal velocities, $v_r$ is the electron or the (equal) ion radial velocity, and $V_r$ and $V_\vartheta$ are the components of the neutral velocity. Also, $\nu_{ei}$ is the electron-ion collision frequency, $\nu_{ie}$ the ion-electron collision frequency, $\nu_{eN}$ the electron-neutral collision frequency, and $\nu_{iN}$ the ion-neutral collision frequency. In solving the equations, it is assumed here that there is no anomalous transport due to instabilities.

We note that as force balance was assumed, all inertia terms of the plasma have been omitted. The neglected inertia terms also included drag due to ionization and centripetal forces. We included all ion inertia terms in our previous publication.[26] In later publications,[27–29] ion and electron inertia were included. Neither diamagnetism nor neutral depletion was addressed in these previous publications.[26–29] Inertia terms are important near the wall, where the ion velocity approaches the Bohm velocity, but these terms make little difference in the bulk of the plasma. It was shown in Ref. 27 that ignoring the electron inertia has a large effect on the solution near the wall but has little effect on the solution of

the problem as a whole. We assume that this holds for the ion inertia as well. Here, we neglect inertia terms and leave for future studies the inclusion in the model of those terms.

We turn to the neutral dynamics. In the radial direction, there is a force balance between the neutral pressure gradient and their collisions with the plasma

$$\frac{\partial(NT_g)}{\partial r} - (nm_i\nu_{iN} + nm_e\nu_{eN})(v_r - V_r) = 0. \tag{5}$$

Here, $N$ is the neutral density and $T_g$ is their temperature. There should be a momentum equation for the neutrals in the azimuthal direction. In the azimuthal direction, the drag by the plasma on the neutrals is balanced by neutral inertia terms. We skip writing the momentum equation for the neutrals in the azimuthal direction as the neutral velocity in the azimuthal direction is assumed to be small.

The collision frequencies are now expressed as $\nu_{iN} = k_{iN}N$, $\nu_{eN} = k_{eN}N$, $\nu_{ei} = k_{ei}n$, and $\nu_{ie} = k_{ie}n$, where $k_{iN}$, $k_{eN}$, $k_{ei}$, and $k_{ie}$ are collision rate constants. Since the net particle flux density is zero, the radial plasma particle flux density, $\Gamma = nv_r$, is related to the radial neutral particle flux density, $\Gamma_N = NV_r$, as

$$\Gamma_N = -\Gamma. \tag{6}$$

The drag term in Eq. (5) can be expressed as $(m_ik_{iN} + m_ek_{eN})\Gamma(N + n)$ and similarly the other drag terms. It is now assumed that $|V_r|$ is much smaller than $v_r$ or, equivalently, that $N$ is much larger than $n$. These inequalities are not always strictly satisfied, but for simplicity, they are used through the numerical solutions here. The neutral velocity components $V_\vartheta$ and $V_r$ are thus neglected in the above equations.

By adding Eqs. (3) and (4), we obtain that $m_e\nu_{eN}v_{e\vartheta} + m_i\nu_{iN}v_{i\vartheta} = 0$. Since $m_ek_{eN} \ll m_ik_{iN}$, it follows that $v_{i\vartheta} \ll v_{e\vartheta}$. We therefore neglect $v_{i\vartheta}$ relative to $v_{e\vartheta}$. We also neglect $m_ek_{eN}$ relative to $m_ik_{iN}$.

We solve the above momentum equations for $E$, $v_{e\vartheta}$, and $v_r$ and obtain the relations for the plasma particle flux density $\Gamma$

$$\Gamma = -\frac{(T_e + T_i)}{m_i\nu_i(\omega_c\omega_{ci}/\nu_i\nu_e + 1)}\frac{\partial n}{\partial r}. \tag{7}$$

and for the ambipolar electric field

$$neE = \frac{[(\omega_c\omega_{ci}/\nu_i\nu_e)T_i - T_e]}{(\omega_c\omega_{ci}/\nu_i\nu_e + 1)}\frac{\partial n}{\partial r}. \tag{8}$$

We assumed that $T_e$ and $T_i$ are uniform across the discharge. Here, $\omega_c \equiv eB/m_e$ and $\omega_{ci} \equiv eB/m_i$ are the electron and ion cyclotron frequencies, $\nu_e = k_{eN}N + k_{ei}n$, and $\nu_i = \nu_{iN}$. The electron-ion collision rate constant is taken as $k_{ei} = 2.9\times10^{-12}\ln\Lambda T_e^{-3/2}(\mathrm{eV})^{3/2}\,\mathrm{m}^3\,\mathrm{s}^{-1}$, where $\ln\Lambda = 10$. The components of the electron velocity are $v_r = \Gamma/n$, where $\Gamma$ is expressed through Eq. (7), and

$$v_{e\vartheta} = \left(\frac{\omega_c}{\nu_e}\right)v_r. \tag{9}$$

Note that the polarity of the electric field can reverse, even locally, depending on the sign of the numerator of Eq. (8). We assume here that $T_i \ll T_e$ and, moreover, that $(\omega_c\omega_{ci}/\nu_i\nu_e)$ $T_i \ll T_e$, so that the electric field points radially outward, namely, pushes the ions towards the wall, the same direction as without the magnetic field. However, the electric field is expected to be weaker when electrons are magnetized, as it is the magnetic field instead of the electric field that impedes their radial motion.

The momentum equations turn out therefore to be

$$T_e\frac{\partial n}{\partial r} = -m_i\nu_i\left(\frac{\omega_c\omega_{ci}}{\nu_i\nu_e} + 1\right)\Gamma, \tag{10}$$

and

$$T_g\frac{\partial N}{\partial r} = m_ik_{iN}N\Gamma. \tag{11}$$

To the momentum equations, we add the continuity equation for the plasma

$$\frac{1}{r}\frac{\partial(r\Gamma)}{\partial r} = \beta_{ion}Nn. \tag{12}$$

The volume source term for the plasma is ionization, which is the sink term for the neutrals. The ionization rate coefficient is $\beta_{ion} = \sigma_0 v_{te}\exp(-\epsilon_i/T_e)$,[30] where $v_{te} \equiv (8T_e/\pi m_e)^{1/2}$ is the electron thermal velocity and $\sigma_0 \equiv \pi(e^2/4\pi\epsilon_0\epsilon_i)^2$, with $\epsilon_0$ being the vacuum permittivity and $\epsilon_i$ the ionization energy.

We turn now to the magnetic field. Employing Ampere's law, we write

$$\frac{\partial B}{\partial r} = \mu_0 env_{e,\vartheta}, \tag{13}$$

where $\mu_0$ is the permeability of the vacuum. The contribution of the ions to the diamagnetic current has been neglected since the ion azimuthal velocity is much smaller than the electron azimuthal velocity, as explained above. Using Eq. (9), the gradient of the magnetic field is expressed as

$$\frac{\partial B}{\partial r} = \mu_0 e\frac{\omega_c}{\nu_e}\Gamma. \tag{14}$$

Summing the four equations, while Eq. (14) is multiplied by $B/\mu_0$, we obtain a total pressure balance

$$nT_e + \frac{B^2}{2\mu_0} + NT_g = \frac{B_W^2}{2\mu_0} + N_WT_g. \tag{15}$$

Here, $B_W$ and $n_W$ are the magnetic field and neutral density at the radial wall, where the plasma density is assumed to vanish, $n = 0$. Equation (15) can substitute one of the four other governing equations.

Equations (10), (11), (12), and (14) [or, equivalently, (15)] are the governing equations for $\Gamma$, $n$, $N$, and $B$ as functions of $r \in [0, a]$. Four boundary conditions are needed. Two of the boundary conditions are $\Gamma(0) = 0$ and $n(a) = 0$. For the neutral density, either $N_W$ or $N_T$, the total number of neutrals per unit length, $N_T = \int_0^a 2\pi rNdr$, is specified. For the magnetic field, either $B_W$ or the total magnetic flux, $\Phi_B$, is specified. The total magnetic flux is $\Phi_B = \int_0^a 2\pi rBdr + B_W\pi(R^2 - a^2)$, where $R(\geq a)$ is the radius of the magnetic coil. In certain

experiments, it can be assumed that the magnetic flux does not change when the discharge is ignited, and thus, $\Phi_B = B_i \pi R^2$, where $B_i$ is the magnetic field in the absence of the plasma. The temperatures $T_e$ and $T_g$ are determined by heat equations for the electrons and for the neutrals. Neutral-gas heating has been addressed (see, for example, Refs. 31 and 32). Here, $T_g$ is specified. Also, since upon solving the equations we also specify either $n_0 \equiv n(0)$ or $\Gamma_W \equiv \Gamma(a)$, the electron temperature $T_e$ becomes an eigenvalue that is determined through the solutions of the governing equations. In the solutions in this paper, $N_W$ and $B_W$ are specified (not $N_T$ and $\Phi_B$). Thus, the following relation is also available:

$$n_0 T_e + \frac{B_0^2}{2\mu_0} + N_0 T_g = \frac{B_W^2}{2\mu_0} + N_W T_g. \tag{16}$$

The magnetic field and the neutral density on axis, $B_0 \equiv B(r=0)$ and $N_0 \equiv N(r=0)$, are found in the calculation, while $n_0$ is also specified (or found if, as stated above, $\Gamma_W$ is specified).

## III. DOMINANCE OF THE DIAMAGNETIC EFFECT

We identify here two parameters that determine the dominance of the diamagnetic effect. Equation (15) can be written as

$$P_n + P_B + P_N = P_{BW} + P_{NW}, \tag{17}$$

where $P_n = nT_e$, $P_B = B^2/2\mu_0$, and $P_N = NT_g$ are the plasma, magnetic, and neutral pressures, respectively, while $P_{BW} \equiv P_B(r=a) = B_W^2/2\mu_0$ and $P_{NW} = P_N(r=a) = N_W T_g$. We write equivalently the pressure balance as

$$\Delta P_n = \Delta P_B + \Delta P_N, \tag{18}$$

where $\Delta P_n \equiv n_0 T_e$ (the plasma pressure at the wall is assumed to vanish), $\Delta P_B \equiv (B_W^2 - B_0^2)/2\mu_0$, $\Delta P_N \equiv T_g \Delta N$, and $\Delta N \equiv N_W - N_0$. The change in the plasma pressure radially across the discharge is balanced by the sum of the change in the magnetic pressure due to the plasma diamagnetic current and the neutral pressure due to neutral depletion. The dominance of neutral pressure in balancing the electron pressure was shown in Ref. 27 to lead to Boltzmann equilibrium. As demonstrated in Ref. 14, the diamagnetic effect is expressed by the first term in Eq. (10), while neutral depletion is expressed by the second term in that equation. The change in the magnetic pressure is dominant when

$$\Delta P_B \geq \Delta P_N. \tag{19}$$

We emphasize that these are not the magnetic pressure or neutral pressure themselves that determine which one of them will balance the plasma pressure, but rather these are the changes in these pressures across the discharge. The last equation can be written as

$$\frac{\Delta B}{B_W} \geq \frac{\Delta N}{N_W} \frac{\beta_N}{1 + B_0/B_W}. \tag{20}$$

Here, $\Delta B \equiv B_W - B_0$, and the neutral beta is defined here as

$$\beta_N \equiv \frac{2\mu_0 N_W T_g}{B_W^2}, \tag{21}$$

the ratio of the maximal neutral pressure to maximal magnetic pressure. If inequality (19) is satisfied, so that $\Delta P_B \gg \Delta P_N$, the magnetic pressure only balances the plasma pressure, and

$$\frac{\Delta B}{B_W} \cong 1 - \sqrt{1 - \beta_n}. \tag{22}$$

The plasma beta is defined here as

$$\beta_n \equiv \frac{2\mu_0 n_0 T_e}{B_W^2}, \tag{23}$$

the ratio of the maximal plasma pressure to the maximal magnetic pressure.

Inequality (19) is satisfied, namely, the magnetic pressure is dominant, if the first term on the right hand side (RHS) of Eq. (10) is larger than the second term. This happens if the parameter

$$C_1 \equiv \frac{\omega_c \omega_{ci}}{\nu_i \nu_e}. \tag{24}$$

is larger than unity, $C_1 > 1$. In that case, the contribution of the diamagnetic current to the pressure balance is dominant. When $C_1 < 1$, the change in neutral pressure radially across the discharge is dominant. The changes (or gradients) in the pressures depend on the coupling of the plasma to the magnetic field through the diamagnetic current and to the neutrals through neutral depletion. The parameter $C_1$ expresses the relative size of these couplings,[14] the coupling to the magnetic field over the coupling to the neutrals. We note that $C_1$ is not uniform across the discharge since it is a function of $B$, $N$, and $n$, which vary with $r$. Therefore, inequality (24) may hold in part of the plasma only. The competition between the magnetic and neutral pressures in balancing the plasma pressure is described through calculations in Sec. VI.

The electric field is also affected by $C_1$. From Eq. (8), it is seen that when $T_i$ is negligible, the electric field in the bulk of the plasma is $E \approx T_e/(ea)$ for $C_1 \ll 1$ and is suppressed to $E \approx T_e/(eaC_1)$ for $C_1 \gg 1$.

It is interesting to compare the diamagnetism, the relative change in the magnetic field, to the neutral depletion, the relative change in the neutral density. This is important since if neutrals are depleted from the bulk of the discharge, the discharge may not be sustained. In particular, we would like to find out when

$$\frac{\Delta B}{B_W} \geq \frac{\Delta N}{N_W}. \tag{25}$$

We note that the magnetic pressure can be dominant, so that inequality (19) [or in its form (20)] is satisfied, but, as $\beta_N/(1 + B_0/B_W)$ is smaller than unity, inequality (25) is not satisfied and neutrals are completely depleted. In order to examine the relationship between the relative changes [Eq. (25)], we note that Eqs. (11) and (14) can be written as

$$\frac{\partial \ln N}{\partial r} = \frac{m_i k_{iN}}{T_g}\Gamma, \qquad \frac{\partial \ln B}{\partial r} = \frac{\mu_0 e^2}{m_e \nu_e}\Gamma. \tag{26}$$

In order for inequality (25) to be satisfied, the parameter

$$C_2 \equiv \frac{\mu_0 e^2 T_g}{m_e \nu_e m_i k_{iN}} \tag{27}$$

has to be larger than unity. Note that

$$C_2 = C_1 \frac{\beta_N}{2}\frac{B_W^2}{B^2}. \tag{28}$$

The effect of varying $C_2$ will be discussed in Sec. VI.

## IV. LINEAR ANALYSIS

Before presenting a full numerical solution of the governing equations, we present a simplified linear analysis (which was first presented in Ref. 14).

We assume that the plasma pressure is small, so that neutral depletion and the diamagnetic effect are small, and the variations of the magnetic field and of the neutral density are small. We solve the equations iteratively. To zeroth order, we assume that the magnetic field and the neutral density are constant. The equations are not linear since the electron collision frequency $\nu_e$ depends on the plasma density that varies radially. We nevertheless substitute $n(r) = n_0$ in the expression for $\nu_e$, so that this collision frequency is constant as well across the discharge. The equations in zeroth order are thus linear with constant coefficients. Equations (12) and (10) are combined in a standard way to $(1/r)\partial/\partial r(r\partial n/\partial r) = -[\alpha(C_1+1)/a^2]n$, where $\alpha \equiv \beta_{ion} m_i \nu_i N_W a^2/T_e$ and

$$C_1 = \frac{e^2 B_W^2}{m_e m_i \nu_i \nu_e}. \tag{29}$$

The coefficients $\alpha$ and $C_1$ are taken as constant, and for $\nu_e$, the electron density is taken as $n_0$, as explained above. Using the boundary condition $n(a) = 0$, we write the plasma density and particle flux density as

$$n = n_0 J_0\left(\frac{p_1 r}{a}\right), \qquad \Gamma = \left[\frac{n_0 T_e}{m_i \nu_i a (C_1+1)}\right] p_1 J_1\left(\frac{p_1 r}{a}\right). \tag{30}$$

Here, $J_0$ and $J_1$ are the Bessel functions of zeroth order and first order, and $p_1 = 2.4048$ is the first zero of $J_0$. The resulting solvability condition, $\sqrt{\alpha(C_1+1)} = p_1$, determines the value of the eigenvalue $T_e$. It was shown in Ref. 23 that, if $\nu_e$ varies with $n$, the density profile is more convex than the Bessel function $J_0(p_1 r/a)$.

The perturbed first-order neutral density and magnetic field are obtained using the zeroth order expressions for $n$ and for $\Gamma$. The neutral density is approximately

$$N = N_W - \left[\frac{1}{(C_1+1)}\frac{n_0 T_e}{T_g}\right] J_0\left(\frac{p_1 r}{a}\right). \tag{31}$$

The magnetic field is approximately

$$B = B_W - \left[\frac{C_1}{(C_1+1)}\frac{\mu_0 n_0 T_e}{B_W}\right] J_0\left(\frac{p_1 r}{a}\right). \tag{32}$$

We therefore write

$$\frac{\Delta N}{N_W} = \frac{1}{(C_1+1)}\frac{n_0 T_e}{N_W T_g}; \qquad \frac{\Delta B}{B_W} = \frac{C_1}{(C_1+1)}\frac{\beta_n}{2}. \tag{33}$$

Substituting these expressions into Eq. (20), with $1 + B_0/B_W \cong 2$, we find that, as expected, inequalities (19) and (20) hold when $C_1 \geq 1$. Also, according to (33), the relative change in $B$ is larger than the relative change in $N$ if

$$C_1 \frac{\beta_N}{2} \geq 1. \tag{34}$$

It is easy to verify that $C_2 = C_1\beta_N/2$, so the condition is

$$C_2 = C_1 \frac{\beta_N}{2} \geq 1, \tag{35}$$

as expected.

When $C_1 \gg 1$, the diamagnetic effect is noticeable, $\Delta B/B_W \cong \beta_n/2$, while $\Delta N/N_W \ll n_0 T_e/N_W T_g$, and when $C_1 \ll 1$, the diamagnetic effect is small, $\Delta B/B_W \ll \beta_n/2$, while the change in the neutral pressure across the discharge due to neutral depletion is large and balances the plasma pressure, $\Delta N/N_W \cong n_0 T_e/N_W T_g$.

## V. DIAMAGNETISM VERSUS NEUTRAL DEPLETION

In this section, we present two cases, case A and case B. The magnetic pressure is the same in the two plasma steady-states of the two cases and so is the neutral pressure. However, the neutral temperature in case A is lower than it is in case B, and correspondingly, since the neutral pressure is the same, the neutral density is higher in case A. As a result of the higher neutral density, ion-neutral collisions are more frequent in case A. This is expressed in a lower $C_1$ in case A. The calculation shows that, as expected, neutral depletion is more pronounced in case A than in case B, while diamagnetism is more pronounced in case B.

Let us describe the plasma in cases A and B. An argon plasma in a cylindrical tube of radius $a = 0.1$ m is confined by a magnetic field of $B_W = 50$ G, so that $P_B(r=a) = 9.95$ Pa, while the gas pressure at the wall is $P_N(r=a) = N_W T_g = 4$ Pa. Therefore, $\beta_N \cong 0.4$. For argon, $\epsilon_i = 15.6$ eV and $k_{eN} = 1.3 \times 10^{-13}$ m$^3$ s$^{-1}$.[30] We also use in the calculation for argon $k_{iN} = 6.3 \times 10^{-16}$ m$^3$/s,[30] although, in order to reach an agreement with the experiment, we sometimes used in our previous publication[14] a larger value of $k_{iN}$.

Case A is discussed first. In case A, presented in Figs. 1–4, the gas temperature is $T_g = 300$ K, and the full equations are solved for three plasma densities, $n_0 = 10^{18}$ m$^{-3}$, $n_0 = 6.5 \times 10^{18}$ m$^{-3}$, and $n_0 = 1.3 \times 10^{19}$ m$^{-3}$. It is found that $T_e$ increases with $n_0$, and $T_e$ is 1.8 eV, 1.9 eV, and 2.7 eV for the three plasma densities, respectively. Figure 1 shows the radial profiles of the normalized plasma density for the three plasma densities. For a higher plasma density, the plasma profile is more convex. The dashed line denotes the

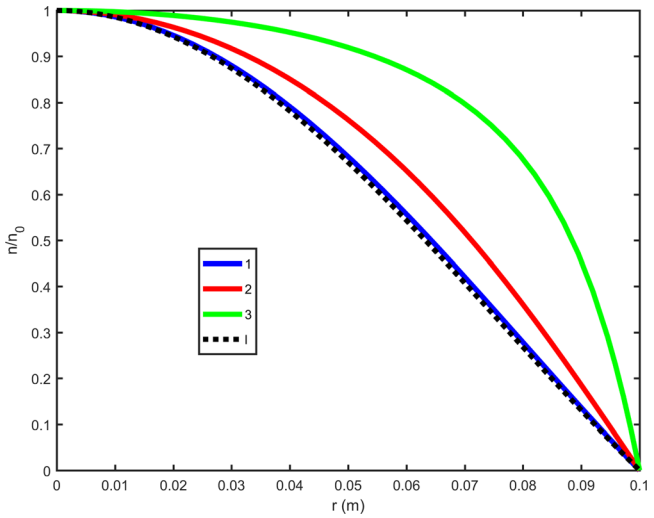


FIG. 1. Case A (argon, $T_g = 300$ K, $P_{NW} = 4$ Pa, $B_W = 50$ G, $a = 0.1$ m). Normalized plasma density profiles $n/n_0$ for three plasma densities are shown: (1) $n_0 = 10^{18}\,\mathrm{m}^{-3}$, (2) $n_0 = 6.5 \times 10^{18}\,\mathrm{m}^{-3}$, and (3) $n_0 = 1.3 \times 10^{19}\,\mathrm{m}^{-3}$. For the lowest density, denoted as 1 (blue–online), the profile coincides with the linear solution (dashed line) [Eq. (30)]. As the plasma density is higher, the profile is more convex.

radial profile of the linear solution [Eq. (30)]. Figure 2 shows the radial profiles of the normalized neutral density for the three plasma densities. As expected, for a higher plasma density, neutral depletion is larger. Figure 3 shows the radial profiles of the magnetic field for the three plasma densities. As expected also here, for a higher plasma density, the diamagnetic effect is larger. The neutral density and the magnetic field obtained by solving the linearized equations are also shown for the three densities in Figs. 2 and 3. It is seen in these figures (and in Fig. 1) that Eqs. (30), (31), and (32) are a good approximation for the profiles of $n$, $N$, and $B$ for the lowest plasma density but are not such a good approximation for the two higher plasma densities.

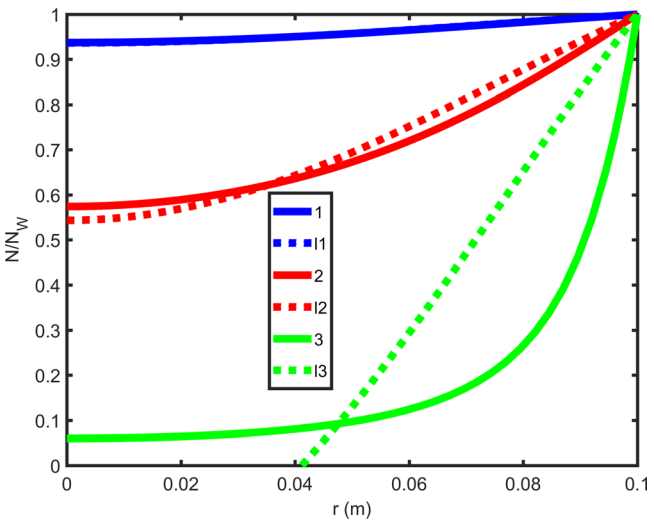


FIG. 2. Case A (argon, $T_g = 300$ K, $P_{NW} = 4$ Pa, $B_W = 50$ G, $a = 0.1$ m). Normalized neutral density profiles $N/N_W$ due to neutral depletion for the three plasma densities as in Fig. 1 are shown. The dotted lines show the approximated expression, Eq. (31), where l1, l2, and l3 denote neutral density profiles for the three plasma densities in an increasing order. The higher the $n_0$ is, the lower the neutral density is.

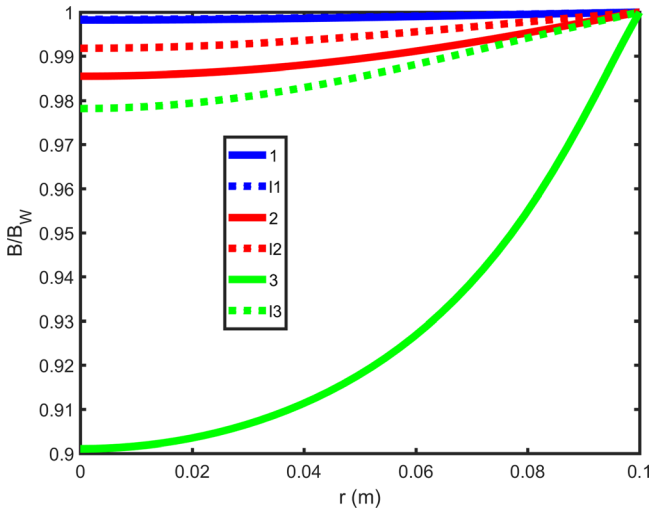


FIG. 3. Case A (argon, $T_g = 300$ K, $P_{NW} = 4$ Pa, $B_W = 50$ G, $a = 0.1$ m). Normalized magnetic field profiles $B/B_W$ due to diamagnetic currents for the three plasma densities as in Fig. 1 are shown. The dotted lines show the approximated expression, Eq. (32), where l1, l2, and l3 denote magnetic field profiles for the three plasma densities in an increasing order. The higher the $n_0$ is, the lower the magnetic field is.

In Figs. 2 and 3, it is seen that $\Delta B/B_W \ll \Delta N/N_W$. For example, for the case of the highest plasma density of the three cases shown, $\Delta B/B_W \cong 0.1$, while $\Delta N/N \cong 0.95$. This larger neutral depletion is in agreement with Eqs. (25) and (27), as $C_2$ is much smaller than unity. Let us show that $C_2$ is smaller than unity. Since $\beta_N \cong 0.4$ and since $B/B_W \approx 1$ for the three densities, it follows from Eq. (35) that $C_2 \simeq 0.2C_1$. The values of $C_1$, defined for $B = B_W$, $n = n_0$, and $N = N_W$, for the three different plasma densities are 0.13, 0.09, and 0.08, so that indeed $C_2 \ll 1$. The relative change in the magnetic field, $\Delta B/B_W \cong 0.1$, is considerably smaller than the value predicted by Eq. (22), which is $1 - \sqrt{1-\beta_n} = 0.19$ (here, $\beta_n = 0.57$).

We now examine the competition between magnetic pressure and neutral pressure in balancing the plasma

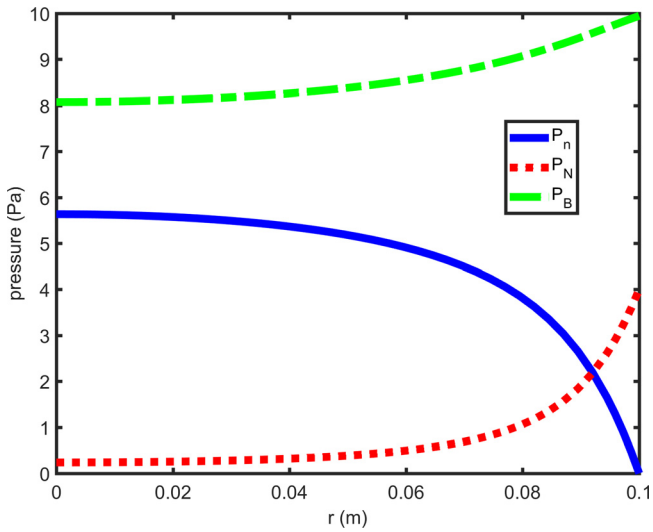


FIG. 4. Case A (argon, $T_g = 300$ K, $P_{NW} = 4$ Pa, $B_W = 50$ G, $a = 0.1$ m). Magnetic pressure $P_B$, neutral pressure $P_N$, and plasma pressure $P_n$ are shown for $n_0 = 1.3 \times 10^{19}\,\mathrm{m}^{-3}$. Neutral pressure is dominant over magnetic pressure: $\Delta P_N > \Delta P_B$.

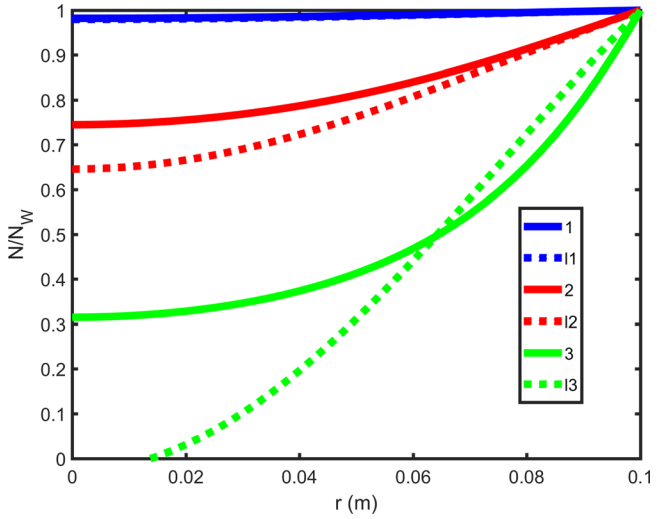


FIG. 5. Case B (argon, $T_g = 1800$ K, $P_{NW} = 4$ Pa, $B_W = 50$ G, $a = 0.1$ m). Normalized neutral density profiles $N/N_W$ due to neutral depletion for three plasma densities are shown: (1) $n_0 = 10^{18}\,\mathrm{m}^{-3}$, (2) $n_0 = 8 \times 10^{18}\,\mathrm{m}^{-3}$, and (3) $n_0 = 1.6 \times 10^{19}\,\mathrm{m}^{-3}$. As in Fig. 2, the dotted lines show the approximated expression, Eq. (31), where l1, l2, and l3 denote neutral density profiles for the three plasma densities in an increasing order. The higher the $n_0$ is, the lower the neutral density is.

pressure in case A. As described above, $C_1 < 1$ for all three plasma densities of case A, and therefore, following Eqs. (19)–(24), the plasma pressure gradient is mostly balanced by the neutral pressure gradient; neutral depletion is dominant. Figure 4 shows the profiles of the various pressures for the highest plasma density, $n_0 = 1.3 \times 10^{19}\,\mathrm{m}^{-3}$. It is seen that $\Delta P_B < 2$ Pa, while $\Delta P_N \cong 4$ Pa.

In case B, shown in Figs. 5–7, the gas pressure is $P_N(r = a) = N_W T_g = 4$ Pa, the same as in case A shown in Figs. 1–4. However, the gas temperature is $T_g = 1800$ K, 6 times higher than in case A, so that the neutral density is 6 times lower. Characteristic values of $C_1$ are 3.7, 1.4, and 1.1 for the three different plasma densities, $n_0 = 10^{18}\,\mathrm{m}^{-3}$, $n_0 = 8 \times 10^{18}\,\mathrm{m}^{-3}$, and $n_0 = 1.6 \times 10^{19}\,\mathrm{m}^{-3}$. The electron temperature $T_e$ increases with $n_0$, and $T_e$ is 2.4 eV, 2.7 eV, and 3.3 eV for the three plasma densities, respectively, higher than in the previous case. Figures 5 and 6 show the radial profiles of the normalized neutral density and magnetic field intensity for the three plasma densities in case B (equivalently to Figs. 2 and 3 of case A). Also, shown in the figures are those radial profiles as found from the linear approximations, which are a good approximation for the lower plasma densities. As expected, and similar to Figs. 2 and 3 of case A, neutral depletion and diamagnetism are larger for a higher plasma density. As is seen in Figs. 5 and 6, in case B, $\Delta B/B_W$ is smaller than $\Delta N/N_W$ as well. However, $(\Delta B/B_W)/(\Delta N/N_W)$ in case B is not as small as it is in case A. Moreover, as $C_1 > 1$ in case B, the plasma pressure is mostly balanced by the magnetic pressure. This is demonstrated in Fig. 7, where $\Delta P_B \cong 6$ Pa, while $\Delta P_N < 3$ Pa.

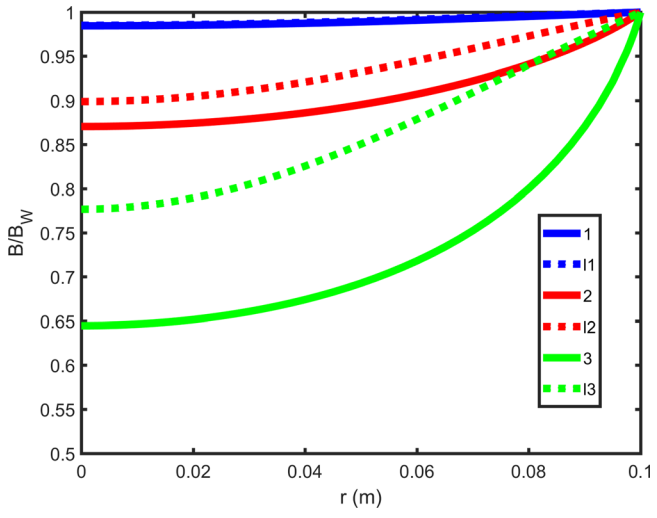


FIG. 6. Case B (argon, $T_g = 1800$ K, $P_{NW} = 4$ Pa, $B_W = 50$ G, $a = 0.1$ m). Normalized magnetic field profiles $B/B_W$ due to diamagnetic currents for the three argon plasma densities and the same parameters as in Fig. 5 are shown. As in Fig. 3, the dotted lines show the approximated expression, Eq. (32), where l1, l2, and l3 denote magnetic field profiles for the three plasma densities in an increasing order. The higher the $n_0$ is, the lower the magnetic field is.

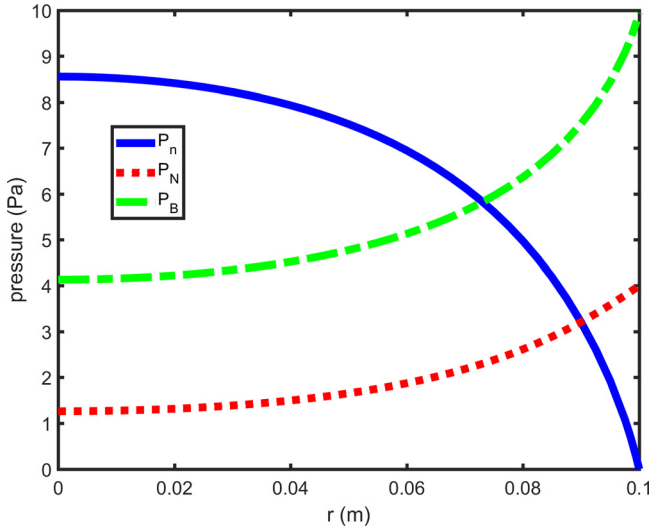


FIG. 7. Case B (argon, $T_g = 1800$ K, $P_{NW} = 4$ Pa, $B_W = 50$ G, $a = 0.1$ m). Magnetic pressure $P_B$, neutral pressure $P_N$, and plasma pressure $P_n$ are shown for $n_0 = 1.6 \times 10^{19}\,\mathrm{m}^{-3}$. The magnetic pressure and neutral pressure at the wall are the same as in Fig. 4, but magnetic pressure is dominant here over neutral pressure, $\Delta P_B > \Delta P_N$.

Figures 1–7, and especially Figs. 4 and 7, in which cases A and B are compared, demonstrate that it is the coupling between the plasma and the neutrals that determines the role of neutrals in suppression of diamagnetism rather than the sizes of the magnetic pressure and neutral pressure themselves. Although the magnetic pressure and the neutral pressure are the same in both cases, in case A, neutral pressure is dominant, while in case B, magnetic pressure is dominant.

## VI. NONMONOTONIC DENSITY DEPENDENCE

In this section, a nonmonotonic dependence of the plasma density $n_0$ on the particle flux $\Gamma_W = \Gamma(r = a)$ is demonstrated. A physical explanation is provided to this somewhat unexpected behavior. In addition, we examine which is larger, the relative change in neutral density $\Delta N/N_W$ or the relative change in the magnetic field $\Delta B/B_W$. As mentioned above, the parameter $C_2$ [defined in Eq. (27)] determines which of the two is dominant. For a larger $C_2$, $(\Delta B/B_W)/(\Delta N/N_W)$ is expected to be larger. The parameter $C_2$ is larger when the gas temperature is higher or when the ion mass is

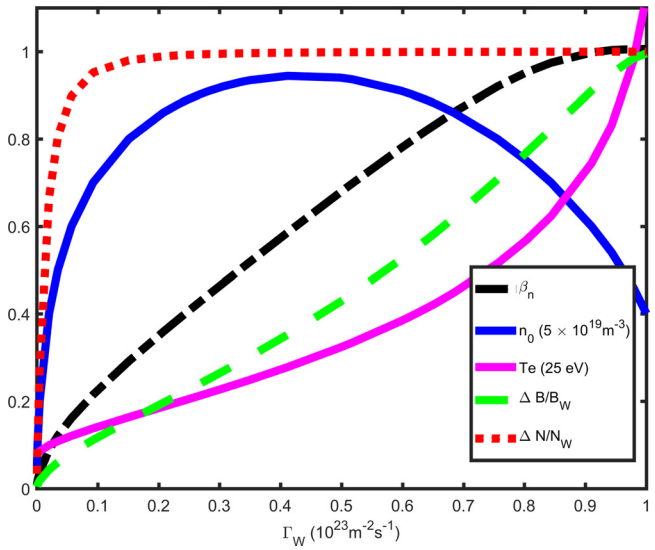


FIG. 8. Case C (argon, $T_g = 300\,\mathrm{K}, P_{NW} = 0.5\,\mathrm{Pa}, B_W = 150\,\mathrm{G}, a = 0.1\,\mathrm{m}$). Electron temperature $T_e$ (solid, magenta), plasma density $n_0$ (solid, nonmonotonic, blue), plasma beta $\beta_n$ (dashed-dotted, black), $\Delta B/B_W$ (dashed, green), and $\Delta N/N_W$ (dotted, red) versus plasma particle flux density $\Gamma_W$ are shown. The nonmonotonic variation of $n_0$ due to the increase in cross-field transport with $\Gamma_W$ is shown; $\Delta N/N_W \gg \Delta B/B_W$.

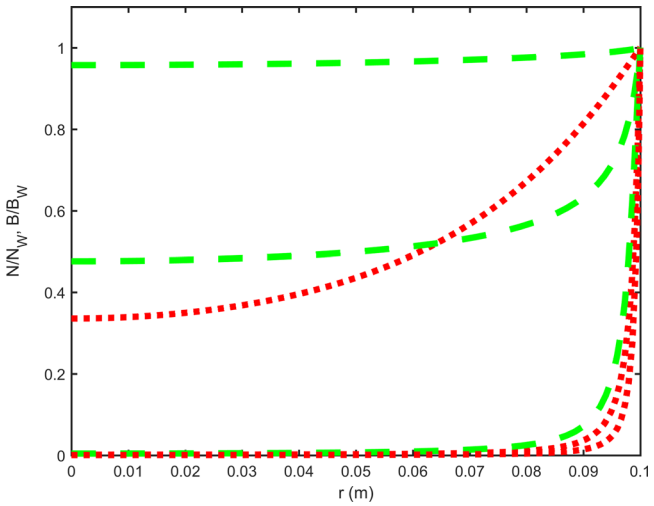


FIG. 10. Case C (argon, $T_g = 300\,\mathrm{K}, P_{NW} = 0.5\,\mathrm{Pa}, B_W = 150\,\mathrm{G}, a = 0.1\,\mathrm{m}$). Radial profiles of $\Delta N/N_W$ (dotted, red) and of $\Delta B/B_W$ (dashed, green) for (1) $\Gamma_W = 2\times10^{21}\,\mathrm{m^{-2}s^{-1}}$ ($n_0 = 2\times10^{19}\,\mathrm{m^{-3}}, T_e = 2.5\,\mathrm{eV}$), (2) $\Gamma_W = 6\times10^{22}$ $\mathrm{m^{-2}s^{-1}}$ ($n_0 = 4.55\times10^{19}\,\mathrm{m^{-3}}, T_e = 9.6\,\mathrm{eV}$), and (3) $\Gamma_W = 1\times10^{23}\,\mathrm{m^{-2}s^{-1}}$ ($n_0$ &132#=$2\times10^{19}$ $\mathrm{m^{-3}}$, $T_e = 28\,\mathrm{eV}$) are shown. As $\Gamma_W$ is larger, $\Delta N/N_W$ and $\Delta B/B_W$ are larger. $\Delta N/N_W \gg \Delta B/B_W$, except for the highest $\Gamma_W$ when both $\Delta N/N_W$ and $\Delta B/B_W$ are close to unity. Neutral depletion is much more pronounced than the diamagnetic effect.

smaller. We calculate the steady states for three different discharges, for which $C_2$ is different. Case C is of argon discharge with gas at room temperature. Case D is of the lighter helium at room temperature, and case E is of helium of a higher gas temperature. It is shown that indeed $(\Delta B/B_W)/(\Delta N/N_W)$ is the largest in case E and the smallest in case C.

In all three cases, C, D, and E, the discharge is in a cylindrical tube of radius $a = 0.1\,\mathrm{m}$, and the plasma is confined by an axial magnetic field, as in the cases A and B. In cases C, D, and E, however, the magnetic field is $B_W = 150\,\mathrm{G}$, higher than in cases A and B, so that the magnetic pressure here is $P_{BW} = 90\,\mathrm{Pa}$. The gas pressure is $P_{NW} = N_W T_g = 0.5\,\mathrm{Pa}$, lower than in cases A and B. Therefore, $P_B \gg P_N$ and $\beta_N = 0.0056$. Moreover, for these parameter values in cases C, D, and E, it turns out that $C_1 \gg 1$, so that the plasma pressure is expected to be balanced mostly by the gradient of the magnetic pressure. Therefore, it follows that in cases C, D, and E presented in Figs. 8–14, $\Delta B/B_W \cong 1 - \sqrt{1-\beta_n}$ (this relation is not shown in the figures). Although $C_1 \gg 1$, it is not clear whether $C_2$ is large as well. Indeed, $C_2$ is different for cases C, D, and E, and as a result, $(\Delta B/B_W)/(\Delta N/N_W)$ is also different in the three cases.

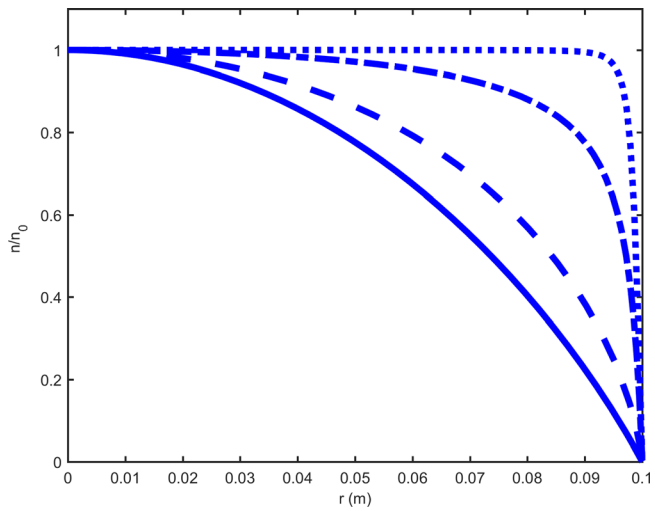


FIG. 9. Case C (argon, $T_g = 300\,\mathrm{K}$, $P_{NW} = 0.5\,\mathrm{Pa}$, $B_W = 150\,\mathrm{G}$, and $a = 0.1\,\mathrm{m}$). Radial profiles of plasma density $n/n_0$ for various plasma particle flux densities $\Gamma_W$ are shown. The most concave profile is at the linear limit: (1) $\Gamma_W = 5\times10^{19}\,\mathrm{m^{-2}\,s^{-1}}$ ($n_0 = 2.5\times10^{18}\,\mathrm{m^{-3}}$, $T_e = 1.9$ eV, negligible diamagnetism and neutral depletion)—solid. The other three profiles are as follows: (2) $\Gamma_W = 2\times10^{21}\,\mathrm{m^{-2}\,s^{-1}}$ ($n_0 = 2\times10^{19}\,\mathrm{m^{-3}}, T_e = 2.5\,\mathrm{eV}$)—dashed, (3) $\Gamma_W = 6\times10^{22}\,\mathrm{m^{-2}\,s^{-1}}$ ($n_0 = 4.55\times10^{19}\,\mathrm{m^{-3}}, T_e = 9.6\,\mathrm{eV}$)—dashed-dotted, and (4) $\Gamma_W = 1\times10^{23}\,\mathrm{m^{-2}\,s^{-1}}$ ($n_0 = 2\times10^{19}\,\mathrm{m^{-3}}, T_e = 28\,\mathrm{eV}$)—dotted. As $\Gamma_W$ is larger, the plasma density profile is more convex.

We start with case C, an argon discharge with $T_g = 300\,\mathrm{K}$. Figures 8–10 describe the calculations for case C. The above-mentioned unexpected nonmonotonic variation of the plasma density with the plasma particle flux density is shown in Fig. 8. We note that $\Gamma_W$, the plasma particle flux density, also represents the rate of plasma generation through Eq. (12). At lower values of $\Gamma_W$, an increase in $\Gamma_W$ results in an increase in $n_0$, the plasma density, as expected. However, for higher $\Gamma_W$, the plasma density decreases with the increase in $\Gamma_W$. This unexpected nonmonotonic dependence of the plasma density on the plasma particle flux density is a result of a varying cross-field transport. The plasma density is determined by both the generation rate (expressed in the flux density $\Gamma_W$) and by the residence time of the plasma in the discharge volume. The residence time is shorter as cross-field transport is faster. At low values of $\Gamma_W$ and when the diamagnetic effect is small, an increase in the generation rate of the plasma (and of $\Gamma_W$) results in a higher plasma density. However, when the plasma generation rate is high, the significant diamagnetic effect results in a lower magnetic field and a faster cross-field transport. The

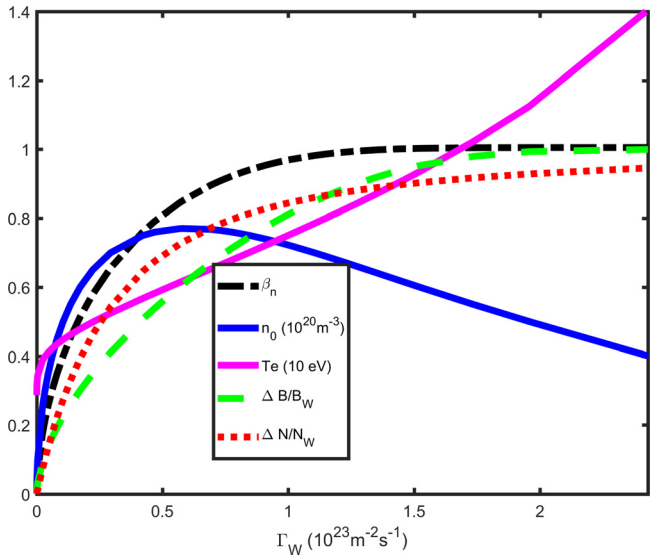


FIG. 11. Case D (helium, $T_g = 300$ K, $P_{NW} = 0.5$ Pa, $B_W = 150$ G, and $a = 0.1$ m). Electron temperature $T_e$ (solid, magenta), plasma density $n_0$ (solid, nonmonotonic, blue), plasma beta $\beta_n$ (dashed-dotted, black), $\Delta B/B_W$ (dashed, green), and $\Delta N/N_W$ (dotted, red) versus plasma particle flux density $\Gamma_W$ are shown. The nonmonotonic variation of $n_0$ due to the increase in cross-field transport with $\Gamma_W$ is shown; $\Delta N/N_W$ and $\Delta B/B_W$ are similar in magnitude.

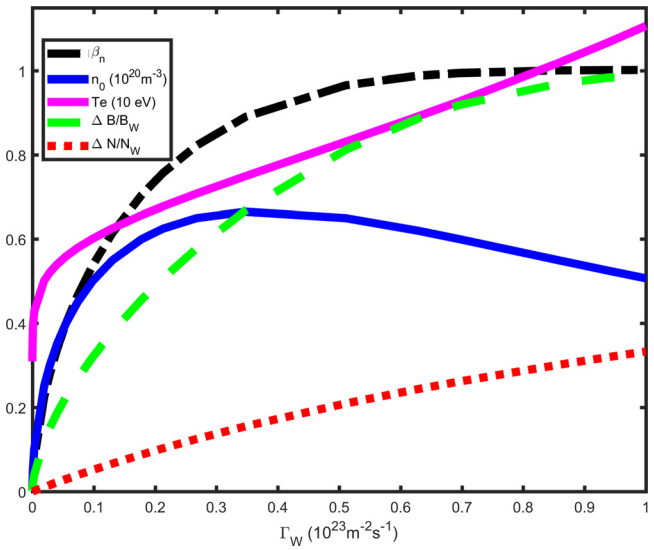


FIG. 13. Case E (helium, $T_g = 1800$ K, $P_{NW} = 0.5$ Pa, $B_W = 150$ G, and $a = 0.1$ m). Electron temperature $T_e$ (solid, magenta), plasma density $n_0$ (solid, nonmonotonic, blue), plasma beta $\beta_n$ (dashed-dotted, black), $\Delta B/B_W$ (dashed, green), and $\Delta N/N_W$ (dotted, red) versus plasma particle flux density $\Gamma_W$ are shown. The nonmonotonic variation of $n_0$ due to the increase in cross-field transport with $\Gamma_W$ is shown; $\Delta B/B_W \gg \Delta N/N_W$.

residence time of the plasma becomes shorter. As a result, the plasma density decreases. It is somewhat counter-intuitive behavior—although more plasma is generated, the plasma density is lower.

A nonmonotonic dependence of the plasma density on the plasma particle flux was also found in an unmagnetized plasma.[22] The reason for the nonmonotonic dependence was similar. The plasma residence time was shorter and the transport was faster for a high plasma particle flux. Neutral depletion decreased the number of neutrals and weakened the drag on the ions. In the previous case,[22] it was neutral depletion that allowed faster plasma transport to the wall, while in our case here, it is plasma diamagnetism that allows such a fast transport.

As is seen in Fig. 8, the plasma beta, $\beta_n$, increases with $\Gamma_W$. As $\Gamma_W$ increases, the plasma density $n_0$ decreases and the temperature $T_e$ increases, so that $\beta_n$, which is proportional to $n_0 T_e$, gets closer to unity.

As $\Gamma_W$ increases, both diamagnetism and neutral depletion increase; $\Delta B/B_W$ and $\Delta N/N_W$ increase and eventually reach unity. However, neutral depletion is dominant, and $\Delta N/N_W$ is much larger than $\Delta B/B_W$. Neutral density, $\Delta N/N_W$,

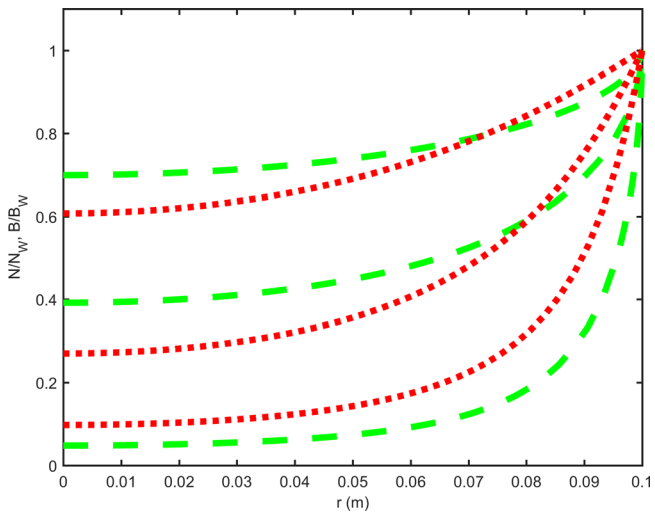


FIG. 12. Case D (helium, $T_g = 300$ K, $P_{NW} = 0.5$ Pa, $B_W = 150$ G, $a = 0.1$ m). Radial profiles of $\Delta N/N_W$ (dotted, red) and of $\Delta B/B_W$ (dashed, green) are shown. Three plasma particle flux densities are as follows: (1) $\Gamma_W = 1.7 \times 10^{22}$ m$^{-2}$ s$^{-1}$ ($n_0 = 6 \times 10^{19}$ m$^{-3}$, $T_e = 4.8$ eV), (2) $\Gamma_W = 5.8 \times 10^{22}$ m$^{-2}$ s$^{-1}$ ($n_0 = 7.7 \times 10^{19}$ m$^{-3}$, $T_e = 6.2$ eV), and (3) $\Gamma_W = 1.5 \times 10^{23}$ m$^{-2}$ s$^{-1}$ ($n_0 = 6 \times 10^{19}$ m$^{-3}$, $T_e = 9.3$ eV). $\Delta B/B_W$ is comparable here to $\Delta N/N_W$. Neutral depletion is comparable to the diamagnetic effect.

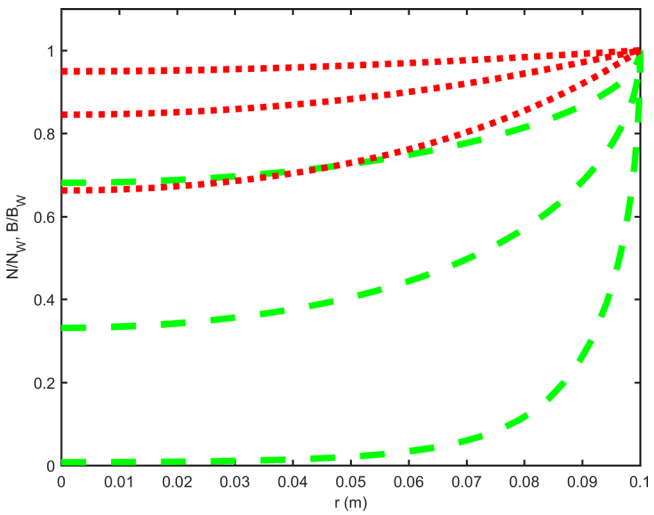


FIG. 14. Case E (helium, $T_g = 1800$ K, $P_{NW} = 0.5$ Pa, $B_W = 150$ G, and $a = 0.1$ m). Radial profiles of $\Delta N/N_W$ (dotted, red) and of $\Delta B/B_W$ (dashed, green). Three plasma particle flux densities are as follows: (1) $\Gamma_W = 9.8 \times 10^{21}$ m$^{-2}$ s$^{-1}$ ($n_0 = 5 \times 10^{19}$ m$^{-3}$, $T_e = 6$ eV), (2) $\Gamma_W = 3.5 \times 10^{22}$ m$^{-2}$ s$^{-1}$ ($n_0 = 6.65 \times 10^{19}$ m$^{-3}$, $T_e = 7.5$ eV), and (3) $\Gamma_W = 1.0 \times 10^{23}$ m$^{-2}$ s$^{-1}$ ($n_0 = 5 \times 10^{19}$ m$^{-3}$, $T_e = 11.2$ eV). $\Delta B/B_W \gg \Delta N/N_W$. The diamagnetic effect is stronger than neutral depletion.

gets closer to unity at much smaller $\Gamma_W$ than diamagnetism, $\Delta B/B_W$, does. As is seen in Fig. 8, $\Delta N/N_W$ is nearly unity already for $\Gamma_W = 5 \times 10^{21}\,\mathrm{m^{-2}\,s^{-1}}$, while $\Delta B/B_W \simeq 0.02$ at that flux density and becomes nearly unity for $\Gamma_W \cong 10^{23}\,\mathrm{m^{-2}\,s^{-1}}$ only. This larger neutral depletion is a result of $C_2$ being smaller than unity everywhere except very close to the wall. This relationship between neutral depletion and diamagnetism in case C can be explained. Often, and also here, $k_{ei}n_0 > k_{eN}N_W$, so that $\nu_e \cong k_{ei}n_0$. From Eq. (27), it can be seen that in such a case, for $C_2$ to be larger than unity, so that $\Delta B/B_W > \Delta N/N_W$, the plasma density has to satisfy $n_0 < \mu_0 e^2 T_g/(m_e k_{ei} m_i k_{iN})$. In case C, of argon with gas at room temperature, the inequality is reduced to $n_0 < 1.2 \times 10^{17}\,\mathrm{m^{-3}}\,T_e^{3/2}(\mathrm{eV})^{-3/2}$. Taking into account electron-neutral collisions would mean that the plasma density has to be even smaller. For $B_W = 150\,\mathrm{G}$ and $T_e$ of few eV, the requirement on the plasma density means that $\beta_n$ has to be much smaller than unity, so that $\Delta B/B_W$ be comparable to $\Delta N/N_W$. However, a necessary condition for $\Delta B/B_W$ to be noticeable is that $\beta_n$ is on the order of unity. Therefore, for the parameters of case C, when $\Delta B/B_W$ is noticeable, $C_2 < 1$, and $\Delta B/B_W$ is smaller than $\Delta N/N_W$, as demonstrated in Fig. 8.

The radial profiles of the normalized plasma density $n/n_0$ are shown in Fig. 9, and normalized neutral density $N/N_W$ and magnetic field $B/B_W$ are shown in Fig. 10, all in case C, for three plasma particle flux densities, $\Gamma_W = 2 \times 10^{21}\,\mathrm{m^{-2}\,s^{-1}}$, $6 \times 10^{22}\,\mathrm{m^{-2}\,s^{-1}}$, and $1 \times 10^{23}\,\mathrm{m^{-2}\,s^{-1}}$. The plasma densities that correspond to the three flux densities are $n_0 = 2 \times 10^{19}\,\mathrm{m^{-3}}$, $4.5 \times 10^{19}\,\mathrm{m^{-3}}$, and again $2 \times 10^{19}\,\mathrm{m^{-3}}$, respectively. The electron temperatures are $T_e = 2.5\,\mathrm{eV}$, 9.6, and 28 eV, respectively. Also, shown in Fig. 9 is the plasma density profile (the most concave) for $\Gamma_W (= 5 \times 10^{19}\,\mathrm{m^{-2}\,s^{-1}})$ that is so low that diamagnetism and neutral depletion are negligible. For this low $\Gamma_W$, the maximal plasma density is $n_0 = 2.5 \times 10^{18}\,\mathrm{m^{-3}}$ and $T_e = 1.9\,\mathrm{eV}$. For this low $\Gamma_W$, the neutral density and magnetic field are uniform and thus are not shown in Fig. 10. As $\Gamma_W$ is higher, the plasma density profile in Fig. 9 is more convex and the neutral density and magnetic field are lower. As was also clear from Fig. 8, neutral depletion is much more pronounced than the diamagnetic effect, $\Delta N/N_W \gg \Delta B/B_W$, except for the highest $\Gamma_W$ when both $\Delta N/N_W$ and $\Delta B/B_W$ are close to unity. Note that, because of the nonmonotonic dependence of the plasma density, the first curve (second for $n/n_0$) and the third curve (fourth for $n/n_0$) are for the same plasma density, $n_0 = 2 \times 10^{19}\,\mathrm{m^{-3}}$. However, the first curve corresponds to low temperature, $T_e = 2.5\,\mathrm{eV}$, low beta, and low diamagnetism and neutral depletion, while the third curve corresponds to high temperature, $T_e = 28\,\mathrm{eV}$, $\beta_n \cong 1$, and high diamagnetism and neutral depletion. The magnetic field and neutrals are actually expelled by the high beta plasma when neutral depletion and diamagnetism are high.

We should note that when the magnetic field and neutrals are expelled almost completely from the plasma, our model for a magnetized plasma ceases to be valid. Nevertheless, the general behavior is still captured by the model.

In cases D and E, the gas is helium. For helium, $\epsilon_i = 24.6\,\mathrm{eV}$, $k_{eN} = 4.54 \times 10^{-14}\,\mathrm{m^3\,s^{-1}}$ (page 62 in Ref. 30 and the polarizabilities from https://www.britannica.com/science/noble-gas), and $k_{iN} = 3.15 \times 10^{-16}\,\mathrm{m^3/s}$ (estimate from page 77 in Ref. 30). As said above, the magnetic field and the gas pressure are the same for the three cases C, D, and E. The magnetic field is $B_W = 150\,\mathrm{G}$, so that $P_{BW} = 90\,\mathrm{Pa}$, and the helium gas pressure is $P_{NW} = 0.5\,\mathrm{Pa}$; therefore, as in C, $P_B \gg P_N$ and $\beta_N = 0.0056$. The parameter $C_1$ in the helium discharge is likely to be larger than in the argon discharge since the ion mass is ten times smaller and $k_{iN}$ is about twice smaller. Therefore, $C_1 \gg 1$, and the plasma pressure in cases D and E is expected to be balanced mostly by the gradient of the magnetic pressure, as it was in case C. The relation $\Delta B/B_W \cong 1 - \sqrt{1-\beta_n}$ also holds in Figs. 11–14, which describe the calculations for cases D and E of helium. The parameter $C_2$ in the helium discharge is also likely to be larger than in the argon discharge, and therefore, $\Delta B/B_W$ is not likely to be that much smaller than $\Delta N/N_W$, as it was for argon plasma of case C.

The calculations of case D, helium discharge where the gas is at room temperature ($T_g = 300\,\mathrm{K}$), are described in Figs. 11 and 12. It is seen in Fig. 11 that, as $\Gamma_W$ increases, both diamagnetism and neutral depletion increase; both $\Delta B/B_W$ and $\Delta N/N_W$ increase and eventually reach unity. However, contrary to the argon discharge of case C, in the helium discharge, diamagnetism and neutral depletion are comparable. This is a result of $C_2$ being closer to unity. A nonmonotonic dependence of $n_0$ on $\Gamma_W$ also occurs for helium. For high $\Gamma_W$, as $\Gamma_W$ increases, $n_0$ decreases, while $T_e$ keeps increasing, so that $\beta_n$ gets closer to unity. It is noted that $T_e$ is generally higher in the helium discharge than in the argon discharge because of the higher ionization energy. Indeed, at the limit of negligible diamagnetism and neutral depletion, $T_e = 2.89\,\mathrm{eV}$ for helium and only 1.9 eV for argon. However, neutral depletion is larger in argon than in helium, and in order to maintain high ionization despite the lower neutral density, $T_e$ in argon turns out to be higher (see Figs. 8 and 11).

Figure 12 shows the radial profiles of $\Delta B/B_W$ and of $\Delta N/N_W$ in case D for three plasma particle flux densities, $\Gamma_W = 1.7 \times 10^{22}\,\mathrm{m^{-2}\,s^{-1}}$, $5.8 \times 10^{22}\,\mathrm{m^{-2}\,s^{-1}}$, and $1.5 \times 10^{23}\,\mathrm{m^{-2}\,s^{-1}}$. The plasma densities that correspond to the three flux densities are $n_0 = 6 \times 10^{19}\,\mathrm{m^{-3}}$, $7.7 \times 10^{19}\,\mathrm{m^{-3}}$, and again $6 \times 10^{19}\,\mathrm{m^{-3}}$, respectively. The electron temperatures are $T_e = 4.8\,\mathrm{eV}$, 6.2 eV, and 9.3 eV, respectively. Neutral depletion is comparable to the diamagnetic effect, $\Delta N/N_W \simeq \Delta B/B_W$. Note that, because of the nonmonotonic dependence of the plasma density, the first curve and the third curve (fourth for $n/n_0$) are for the same plasma density, $n_0 = 6 \times 10^{19}\,\mathrm{m^{-3}}$. However, the first curve corresponds to low temperature, $T_e = 4.8\,\mathrm{eV}$, low beta, and low diamagnetism and neutral depletion, while the third curve corresponds to high temperature, $T_e = 9.3\,\mathrm{eV}$, high beta, and high diamagnetism and neutral depletion. Such two different steady state plasmas with the same plasma density $n_0$, which are shown here for case D, were also pointed out in Figs. 8–10 for argon (case C). The radial profiles of the plasma density for the three $\Gamma_W$ are not shown for case D since they are similar to those shown in Fig. 9 for case C.

Figures 13 and 14 describe the calculations for case E, helium discharge where the gas is at a higher temperature of

1800 K (and a lower neutral gas density to keep neutral pressure the same as in cases C and D). From Eq. (27), it is seen that $C_2$ is larger for a higher gas temperature. This leads, as is shown in the figures, to the diamagnetic effect being more pronounced than in the previous examples of argon and helium at room temperature (cases C and D). Moreover, the diamagnetic effect is actually stronger than neutral depletion in this case, $\Delta B/B_W \gg \Delta N/N_W$. It is seen in Fig. 13, similar to Figs. 8 and 11, that, as $\Gamma_W$ increases, both diamagnetism and neutral depletion increase. A nonmonotonic dependence of $n_0$ on $\Gamma_W$ also occurs for helium at this higher gas temperature. For high $\Gamma_W$, as $\Gamma_W$ increases, $n_0$ decreases, while $T_e$ keeps increasing, and $\beta_n$ gets closer to unity.

Figure 14 shows the radial profiles of the normalized neutral density $N/N_W$ and of magnetic field $B/B_W$ in case E. Three plasma particle flux densities are $\Gamma_W = 9.8 \times 10^{21}\,\mathrm{m^{-2}\,s^{-1}}$, $3.5 \times 10^{22}\,\mathrm{m^{-2}\,s^{-1}}$, and $1.0 \times 10^{23}\,\mathrm{m^{-2}\,s^{-1}}$. The corresponding plasma densities are $n_0 = 5 \times 10^{19}\,\mathrm{m^{-3}}$, $6.65 \times 10^{19}\,\mathrm{m^{-3}}$, and again $5 \times 10^{19}\,\mathrm{m^{-3}}$, respectively. The electron temperatures are $T_e = 6\,\mathrm{eV}$, 7.5, and 11 eV. The plasma density profiles are not shown as they are similar to those of case C shown in Fig. 9. Here, $\Delta B/B_W \gg \Delta N/N_W$. The diamagnetic effect is stronger than neutral depletion.

In this section, a nonmonotonic variation of the plasma density with the plasma particle flux density was demonstrated and explained. Neutral depletion and diamagnetism were compared for three different cases. A dimensionless parameter was identified, which determines which of the two processes is dominant.

## VII. THE EFFECT OF THE MAGNETIC FIELD INTENSITY

In this section, we examine how diamagnetism and neutral depletion vary with the intensity of the applied magnetic field. The variation depends on the plasma parameters that are varied or are kept constant. If the plasma density $n_0$ is kept constant when the magnetic field increases, it is likely that diamagnetism, $\Delta B/B_W$, decreases because the plasma beta $\beta_n$ decreases. Neutral depletion, $\Delta N/N_W$, is also expected to decrease with an increase in the magnetic field in that case, as was explained in Ref. 24. Here, we examine the effect of the variation of the magnetic field in two cases. In the first case, case F, the magnetic field $B_W$ is varied, while the maximal plasma density $n_0$ is indeed kept constant, as was discussed earlier.[24] In the second case, case G, $B_W$ is varied, while $\Gamma_W$ is kept constant. It is shown here that in case G, neutral depletion, $\Delta N/N_W$, does not decrease with the magnetic field $B_W$, but rather it is approximately constant. We comment that case G, in which $\Gamma_W$ is kept constant, corresponds roughly to keeping the deposited power in the plasma constant (this is only approximate since as $T_e$ changes, the energy cost changes,[33,34] and therefore, for the same power, $\Gamma_W$ does change). Our purpose in this section is therefore to demonstrate numerically the different behavior of neutral depletion in the two cases, F and G, and to explain the different behavior qualitatively.

The dependence of diamagnetism on the magnetic field intensity was studied experimentally and modelled theoretically in Ref. 14. However, it was difficult in the experiment to vary the magnetic field while keeping either plasma density or plasma particle flux density constant. We study this issue theoretically here.

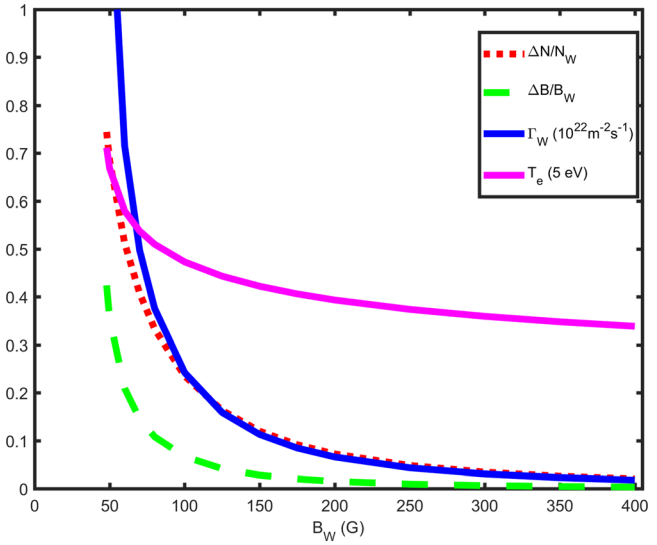


FIG. 15. Case F (argon, $T_g = 1800\,\mathrm{K}$, $P_{NW} = 4\,\mathrm{Pa}$, $B_W = 150\,\mathrm{G}$, and $a = 0.1\,\mathrm{m}$). The maximal plasma density is fixed: $n_0 = 1.6 \times 10^{19}\,\mathrm{m^{-3}}$. Electron temperature $T_e$ (solid, magenta), plasma particle flux density $\Gamma_W$ (solid, blue), $\Delta B/B_W$ (dashed, green), and $\Delta N/N_W$ (dotted, red) versus the magnetic field $B_W$ are shown. Neutral depletion decreases with the magnetic field.

We choose to model an argon discharge in both cases, F and G. The gas pressure is taken as $P_{NW} = 4\,\mathrm{Pa}$, so that the neutral pressure is not negligible relative to the magnetic pressure. In addition, following the examples in Figs. 1–7 (cases A and B), it is assumed that $T_g = 1800\,\mathrm{K}$. As in all the examples, the radius of the cylindrical tube is $a = 0.1\,\mathrm{m}$.

We start by examining the effect of varying the magnetic field intensity $B_W$ while the maximal plasma density $n_0$ is kept constant (case F). Figures 15–17 show the results of the calculation, in which the plasma maximal density is specified as $n_0 = 1.6 \times 10^{19}\,\mathrm{m^{-3}}$.

Figure 15 shows the electron temperature $T_e$, the plasma particle flux density $\Gamma_W$, the relative change in the magnetic field $\Delta B/B_W$, and the relative change in the neutral density $\Delta N/N_W$ versus the magnetic field $B_W$. All these quantities indeed decrease with the magnetic field. In particular, neutral depletion, $\Delta N/N_W$, decreases with $B_W$, as claimed in Ref. 24.

Some of the dependencies on the magnetic field in Fig. 15 can be understood by examining the governing equations. Because of the decrease in $T_e$ with $B_W$, $\Gamma_W$ decreases for a fixed $n_0$, following Eq. (12). Since $\Gamma_W$ decreases, $\Delta N/N_W$ and $\Delta B/B_W$ have to decrease, following Eqs. (11) and (13).

Radial profiles of normalized plasma density $n/n_0$ are shown in Fig. 16 and of normalized neutral density $N/N_W$ and magnetic field $B/B_W$ are shown in Fig. 17 for case F. As in Fig. 15, $n_0 = 1.6 \times 10^{19}\,\mathrm{m^{-3}}$. The profiles are for four magnetic field intensities: $B_W = 50\,\mathrm{G}$ ($\Gamma_W = 1.3 \times 10^{22}\ \mathrm{m^{-2}\,s^{-1}}$, $T_e = 3.3\,\mathrm{eV}$), $60\,\mathrm{G}$ ($\Gamma_W = 7.2 \times 10^{21}\,\mathrm{m^{-2}\,s^{-1}}$, $T_e = 2.9\,\mathrm{eV}$) $70\,\mathrm{G}$ ($\Gamma_W = 4.5 \times 10^{21}\,\mathrm{m^{-2}\,s^{-1}}$, $T_e = 2.7\,\mathrm{eV}$), and $400\,\mathrm{G}$ ($\Gamma_W = 1.8 \times 10^{20}\,\mathrm{m^{-2}\,s^{-1}}$, $T_e = 1.7\,\mathrm{eV}$). As seen in Fig. 17, for a higher $B_W$, the reductions of both $B/B_W$ and $N/N_W$ are

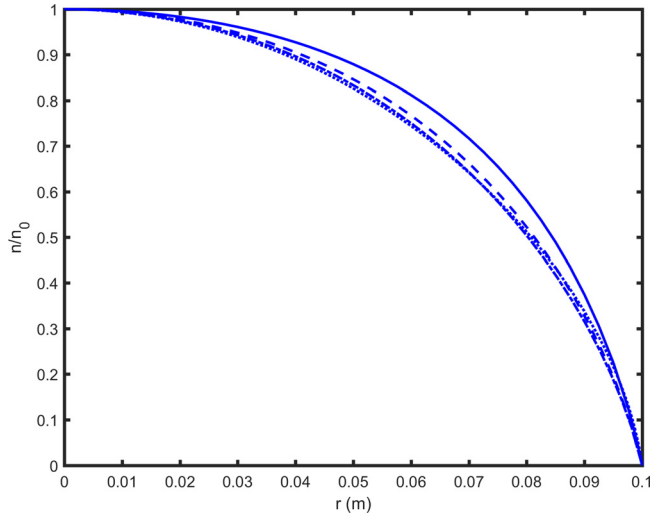


FIG. 16. Case F (argon, $T_g = 1800\,\mathrm{K}$, $P_{NW} = 4\,\mathrm{Pa}$, $B_W = 150\,\mathrm{G}$, and $a = 0.1\,\mathrm{m}$). The maximal plasma density is fixed: $n_0 = 1.6 \times 10^{19}\,\mathrm{m}^{-3}$. Radial profiles of normalized plasma density $n/n_0$ for four magnetic field intensities are as follows: (1) $B_W = 50\,\mathrm{G}\,(\Gamma_W = 1.3 \times 10^{22}\,\mathrm{m}^{-2}\,\mathrm{s}^{-1}$, $T_e = 3.3\,\mathrm{eV}$)—solid, (2) $B_W = 60\,\mathrm{G}\,(\Gamma_W = 7.2 \times 10^{21}\,\mathrm{m}^{-2}\,\mathrm{s}^{-1}, T_e = 2.9\,\mathrm{eV})$—dashed, (3) $B_W = 70\,\mathrm{G}\,(\Gamma_W = 4.5 \times 10^{21}\,\mathrm{m}^{-2}\,\mathrm{s}^{-1}$, $T_e = 2.7\,\mathrm{eV}$)—dashed-dotted, and (4) $B_W = 400\,\mathrm{G}\,(\Gamma_W = 1.8 \times 10^{20}\,\mathrm{m}^{-2}\,\mathrm{s}^{-1}$, $T_e = 1.7\,\mathrm{eV}$)—dotted. The plasma density profile hardly changes with $B_W$. For a lower $B_W$, $n/n_0$ is slightly more convex (for a lower $B_W$, neutral depletion is larger—see Fig. 17).

smaller. It is concluded that neutral depletion indeed decreases with the magnetic field, as claimed in Ref. 24.

We note that the case of $B_W = 50\,\mathrm{G}$ is also included in the examples of Figs. 5–7. We also note that for a lower $B_W$, in which case neutral depletion is larger, $n/n_0$ is slightly more convex. The reasons for $n/n_0$ becoming more or less convex require further study.

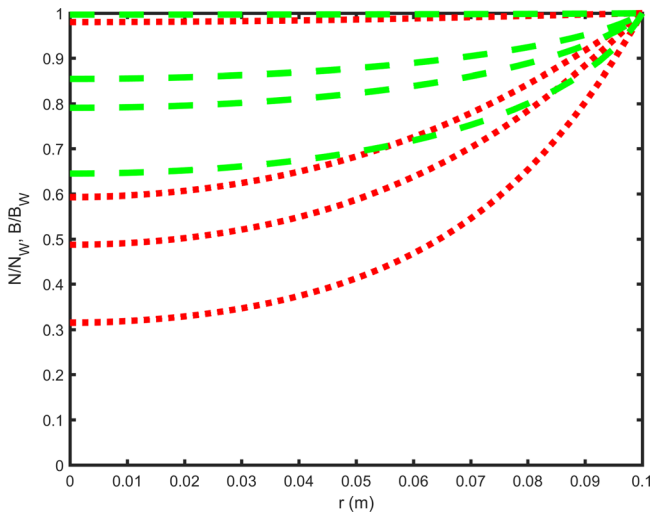


FIG. 17. Case F (argon, $T_g = 1800\,\mathrm{K}$, $P_{NW} = 4\,\mathrm{Pa}$, $B_W = 150\,\mathrm{G}$, $a = 0.1\,\mathrm{m}$). The maximal plasma density is fixed: $n_0 = 1.6 \times 10^{19}\,\mathrm{m}^{-3}$. Radial profiles of normalized neutral density $N/N_W$ (dotted, red) and magnetic field $B/B_W$ (dashed, green) for four magnetic field intensities are shown, as in Fig. 16: (1) $B_W = 50\,\mathrm{G}\,(\Gamma_W = 1.3 \times 10^{22}\,\mathrm{m}^{-2}\,\mathrm{s}^{-1}$, $T_e = 3.3\,\mathrm{eV}$), (2) $B_W = 60\,\mathrm{G}\,(\Gamma_W = 7.2 \times 10^{21}\,\mathrm{m}^{-2}\,\mathrm{s}^{-1}$, $T_e = 2.9\,\mathrm{eV}$), (3) $B_W = 70\,\mathrm{G}\,(\Gamma_W = 4.5 \times 10^{21}\,\mathrm{m}^{-2}\,\mathrm{s}^{-1}$, $T_e = 2.7\,\mathrm{eV}$), and (4) $B_W = 400\,\mathrm{G}$ $(\Gamma_W = 1.8 \times 10^{20}\,\mathrm{m}^{-2}\,\mathrm{s}^{-1}$, $T_e = 1.7\,\mathrm{eV}$). For a higher $B_W$, the decrease in both $B/B_W$ and $N/N_W$ is smaller—diamagnetism and neutral depletion are smaller.

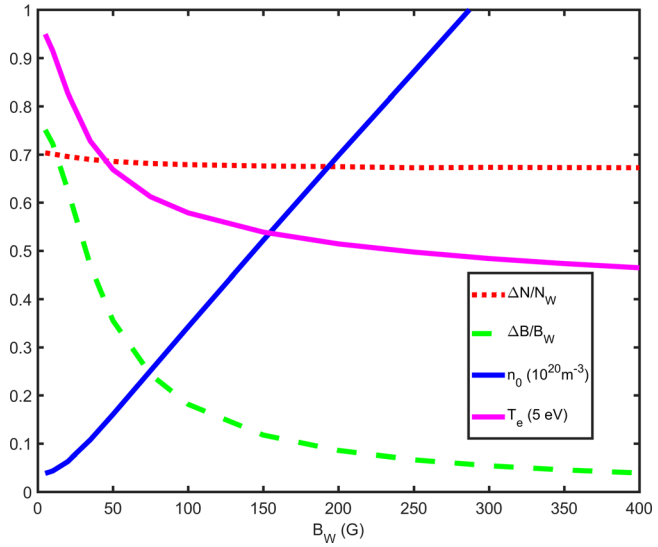


FIG. 18. Case G (argon, $T_g = 1800\,\mathrm{K}$, $P_{NW} = 4\,\mathrm{Pa}, B_W = 150\,\mathrm{G}$, $a = 0.1\,\mathrm{m}$). Plasma particle flux density is fixed: $\Gamma_W = 1.3 \times 10^{22}\,\mathrm{m}^{-2}\,\mathrm{s}^{-1}$. Electron temperature $T_e$ (solid, magenta), plasma particle flux density $\Gamma_W$ (solid, blue), $\Delta B/B_W$ (dashed, green) and $\Delta N/N_W$ (dotted, red) versus the magnetic field $B_W$ are shown. Neutral depletion hardly varies with the magnetic field.

We turn now to examine the effect of varying the magnetic field intensity while the plasma particle flux density at the wall $\Gamma_W$ is kept constant (case G). Figure 18 shows the electron temperature $T_e$, the plasma density $n_0$, the relative changes in the magnetic field $\Delta B/B_W$, and in the neutral density $\Delta N/N_W$ versus the magnetic field $B_W$. The plasma particle flux density at the wall is kept constant, $\Gamma_W = 1.3 \times 10^{22}\,\mathrm{m}^{-2}\,\mathrm{s}^{-1}$, while $B_W$ varies. In this case, neutral depletion hardly varies with the magnetic field. The relative

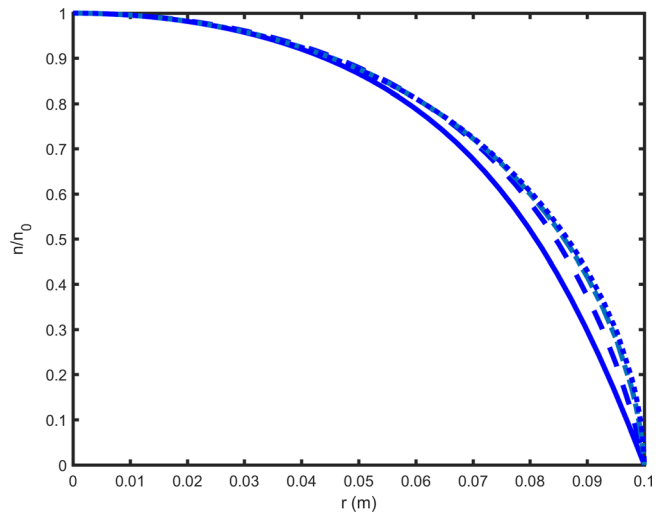


FIG. 19. Case G (argon, $T_g = 1800\,\mathrm{K}$, $P_{NW} = 4\,\mathrm{Pa}, B_W = 150\,\mathrm{G}$, $a = 0.1\,\mathrm{m}$). Plasma particle flux density is fixed: $\Gamma_W = 1.3 \times 10^{22}\,\mathrm{m}^{-2}\,\mathrm{s}^{-1}$. Radial profiles of normalized plasma density $n/n_0$ for four magnetic field intensities are as follows: (1) $B_W = 10\,\mathrm{G}\,(n_0 = 4.3 \times 10^{18}\,\mathrm{m}^{-3}$, $T_e = 4.6\,\mathrm{eV}$)—solid, (2) $B_W = 50\,\mathrm{G}\,(n_0 = 1.6 \times 10^{19}\,\mathrm{m}^{-3}, T_e = 3.3\,\mathrm{eV})$—dashed, (3) $B_W = 150\,\mathrm{G}\,(n_0 = 5.2 \times 10^{19}\,\mathrm{m}^{-3}$, $T_e = 2.7\,\mathrm{eV}$)—dashed-dotted, and (4) $B_W = 350\,\mathrm{G}\,(n_0 = 1.2 \times 10^{20}\,\mathrm{m}^{-3}, T_e = 2.3\,\mathrm{eV})$—dotted. The plasma density profile hardly changes with $B_W$. For a higher $B_W$, $n/n_0$ is slightly more convex.

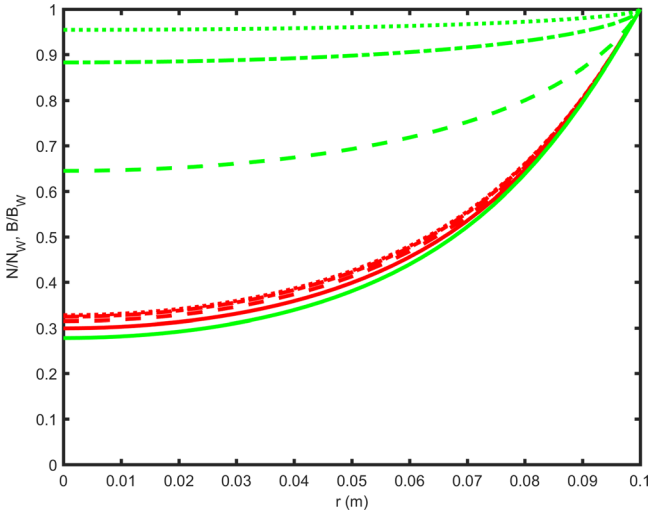


FIG. 20. Case G (argon, $T_g = 1800\,\mathrm{K}, P_{NW} = 4\,\mathrm{Pa}, B_W = 150\,\mathrm{G}, a = 0.1\,\mathrm{m}$). Plasma particle flux density is fixed: $\Gamma_W = 1.3 \times 10^{22}\,\mathrm{m^{-2}\,s^{-1}}$. Radial profiles of normalized neutral density $N/N_W$ (dotted, red) and magnetic field $B/B_W$ (dashed, green) for four magnetic field intensities, are shown as in Fig. 19: (1) $B_W = 10\mathrm{G}\,(n_0 = 4.3 \times 10^{18}\,\mathrm{m^{-3}}, T_e = 4.6\mathrm{eV})$, (2) $50\mathrm{G}\,(n_0 = 1.6 \times 10^{19}\,\mathrm{m^{-3}}$, $T_e = 3.3\mathrm{eV})$, (3) $150\mathrm{G}\,(n_0 = 5.2 \times 10^{19}\,\mathrm{m^{-3}}, T_e = 2.7\mathrm{eV})$, and (4) 350G $(n_0 = 1.2 \times 10^{20}\,\mathrm{m^{-3}}, T_e = 2.3\mathrm{eV})$. For a higher $B_W$, the decrease in $B/B_W$ is smaller (smaller diamagnetism). $N/N_W$ hardly varies with $B_W$, and the decrease in $N/N_W$ is very slightly smaller (a slightly smaller neutral depletion) when $B_W$ is increased.

change in the magnetic field $\Delta B/B_W$ and $T_e$ decreases, while $n_0$ increases approximately linearly with $B_W$.

The dependence on the magnetic field can be understood by examining the governing equations also here for case G. From Eq. (11), it is seen that the relative change in the neutral density is determined by the integral of $m_i k_{iN} \Gamma / T_g$. If $\Gamma_W$ is kept constant, it is expected that neutral depletion will be approximately constant as well. The plasma density is determined by Eq. (10), in which we assume that the first term on the RHS is dominant and that electrons collide mostly with ions, so that $\nu_e \propto n$. If $\Gamma_W$ is kept constant, it is seen that $n \propto B$, although diamagnetism and variation of $T_e$ make the dependence less obvious. The numerical calculations include all these effects. Finally, from Eq. (14), we see that $\Delta B/B_W$ varies as the integral of $\nu_e^{-1}$ for a constant $\Gamma_W$. Since $\nu_e$ is roughly proportional to $n$, it follows that $\Delta B/B_W \propto n^{-1}$. Thus, $n \propto B$ results in $\Delta B/B_W \propto B^{-1}$. Indeed, the dependence seen in Fig. 18 is roughly $\Delta B/B_W \propto B_W^{-1}$.

Radial profiles of normalized plasma density $n/n_0$ are shown in Fig. 19, and neutral density $N/N_W$ and magnetic field $B/B_W$ are shown in Fig. 20, for the same parameters as in Fig. 18 for four magnetic field intensities: $B_W = 10\mathrm{G}\,(n_0 = 4.3 \times 10^{18}\,\mathrm{m^{-3}}$, $T_e = 4.6\mathrm{eV})$, $50\mathrm{G}\,(n_0 = 1.6 \times 10^{19}\,\mathrm{m^{-3}}$, $T_e = 3.3\mathrm{eV})$, $150\mathrm{G}\,(n_0 = 5.2 \times 10^{19}\,\mathrm{m^{-3}}, T_e = 2.7\mathrm{eV})$ and 350G $(n_0 = 1.2 \times 10^{20}\,\mathrm{m^{-3}}, T_e = 2.3\mathrm{eV})$. We note again that the case of $B_W = 50\mathrm{G}$ is also included in the examples of Figs. 5–7. Neutral depletion is almost constant. The profile of neutral density is almost the same for all magnetic field intensities. The neutral density is only slightly higher for a higher $B_W$. Also, the reduction of $B/B_W$ is smaller and $n/n_0$ is more convex for a higher $B_W$. As written above, the reasons for $n/n_0$ becoming more or less convex require further study.

## VIII. CONCLUSIONS

In this paper, we have extended our previous study[14] of diamagnetism and neutral depletion in a magnetized plasma. Both phenomena result from the plasma pressure. We have explored when either magnetic pressure or neutral pressure balances the plasma pressure. We also determined the condition for either the relative change in the magnetic field (due to diamagnetism) or the relative change in the neutral density (due to neutral depletion) to be more pronounced. Two coupling parameters, $C_1$ and $C_2$, that indicate which pressure is dominant in the pressure balance and which relative change is more pronounced, were identified. A nonmonotonic dependence of the plasma maximal density on the plasma particle flux density has been identified and explained. Finally, the effect of the magnetic field on neutral depletion was examined, and it was shown that neutral depletion either decreases or does not vary, depending on whether the plasma density of the plasma particle flux density is kept constant while the magnetic field is increased.

Various assumptions have been made in formulating the model. For various cases, it is needed to relax some of these assumptions. As an example, when neutral depletion is intense, neutral density may become smaller than the plasma density and the model should be modified to account for that.

We should note that for certain applications, it is important that plasma mostly flows axially along magnetic field lines. This is true for helicons used in electric propulsion, for example, Ref. 35. Such cylindrical plasmas with flow mostly axial should be modeled differently.

## ACKNOWLEDGMENTS

The authors are grateful to Dr. D. Kuwahara for useful discussions. A.F. was supported by the Japan Society for the Promotion of Science (JSPS) Invitation Fellowship under Contract No. S14033 and by the Israel Science Foundation, Grant Nos. 765/11 and 1581/16. S.S. was partly supported by NIFS budget code NIFS17KBAP035.

[1]K. Miyamoto, *Plasma Physics for Nuclear Fusion* (The MIT Press, Cambridge, 1979).
[2]D. Leneman, W. Gekelman, and J. Maggs, Phys. Rev. Lett. **82**, 2673 (1999).
[3]M. Ichimura, M. Inutake, T. Katanuma, N. Hino, H. Hojo, K. Ishii, T. Tamano, and S. Miyoshi, Phys. Rev. Lett. **70**, 2734 (1993).
[4]T. Tsurutani, G. S. Lakhina, O. P. Verkhoglyadova, E. Echer, F. L. Guamieri, Y. Narita, and D. O. Constantinescu, J. Geophys. Res. **116**, A02103, http://dx.doi.org/10.1029/2010JA015913 (2011).
[5]R. W. Boswell, Phys. Lett. A **33**, 457 (1970).
[6]E. Scime, P. A. Keiter, M. M. Balkey, R. F. Boivin, J. L. Kline, and M. Blackburn, Phys. Plasmas **7**, 2157 (2000).
[7]R. Stenzel and J. M. Urrutia, Phys. Plasmas **7**, 4450 (2000).
[8]C. S. Corr and R. W. Boswell, Phys. Plasmas **14**, 122503 (2007).
[9]S. Shinohara, T. Motomura, K. Tanaka, T. Tanikawa, and K. P. Shamrai, Plasma Sources Sci. Technol. **19**, 034018 (2010).
[10]B. R. Roberson, R. Winglee, and J. Prager, Phys. Plasmas **18**, 053505 (2011).
[11]K. Takahashi, C. Charles, and R. W. Boswell, Phys. Rev. Lett. **110**, 195003 (2013).
[12]K. Takahashi, A. Chiba, A. Komuro, and A. Ando, Plasma Sources Sci. Technol. **25**, 055011 (2016).
[13]K. Takahashi and A. Ando, Phys. Rev. Lett. **118**, 225002 (2017).

[14]S. Shinohara, D. Kuwahara, K. Yano, and A. Fruchtman, Phys. Plasmas **23**, 122108 (2016).
[15]S. Shinohara, T. Hada, T. Motomura, K. Tanaka, T. Tanikawa, K. Toki, Y. Tanaka, and K. P. Shamrai, Phys. Plasmas **16**, 057104 (2009).
[16]S. Shinohara, S. Takechi, and Y. Kawai, Jpn. J. Appl. Phys., Part 1 **35**, 4503 (1996).
[17]A. Caruso and A. Cavaliere, Brit. J. Appl. Phys. **15**, 1021 (1964).
[18]H.-B. Valentini, Beitr. Plasmaphys. **11**, 483 (1971) (in German, English Abstract).
[19]P. C. Stangeby and J. E. Allen, J. Phys. A: Gen. Phys. **4**, 108 (1971); J. Phys. D: Appl. Phys. **6**, 224 (1973).
[20]J. Gilland, R. Breun, and N. Hershkowitz, Plasma Sources Sci. Technol. **7**, 416 (1998).
[21]S. Cho, Phys. Plasmas **6**, 359 (1999).
[22]A. Fruchtman, G. Makrinich, P. Chabert, and J. M. Rax, Phys. Rev. Lett. **95**, 115002 (2005).
[23]A. Fruchtman, Plasma Sources Sci. Technol. **18**, 025033 (2009).
[24]L. Liard, J.-L. Raimbault, and P. Chabert, Phys. Plasmas **16**, 053507 (2009).
[25]A. Simon, Phys. Rev. **98**, 317 (1955).
[26]A. Fruchtman, G. Makrinich, and J. Ashkenazy, Plasma Sources Sci. Technol. **14**, 152 (2005).
[27]N. Sternberg, V. Godyak, and D. Hoffman, Phys. Plasmas **13**, 063511 (2006).
[28]T. M. G. Zimmermann, M. Coppins, and J. E. Allen, Phys. Plasmas **16**, 043501 (2009).
[29]E. Ahedo, Phys. Plasmas **16**, 113503 (2009).
[30]M. A. Lieberman and A. J. Lichtenberg, *Principles of Plasma Discharges and Materials Processing*, 2nd ed. (Wiley, New York, 2005).
[31]A. Fruchtman, Plasma Sources Sci. Technol. **17**, 024016 (2008).
[32]L. Liard, J.-L. Raimbault, J.-M. Rax, and P. Chabert, J. Phys. D: Appl. Phys. **40**, 5192 (2007).
[33]J. T. Gudmundsson, Report No. RH-21-2002, Science Institute, University of Iceland, Reykjavik, Iceland, 2002.
[34]A. T. Hjartarson, E. G. Thorsteinsson, and J. T. Gudmundsson, Plasma Sources Sci. Technol. **19**, 065008 (2010).
[35]C. Charles, J. Phys. D: Appl. Phys. **42**, 163001 (2009).